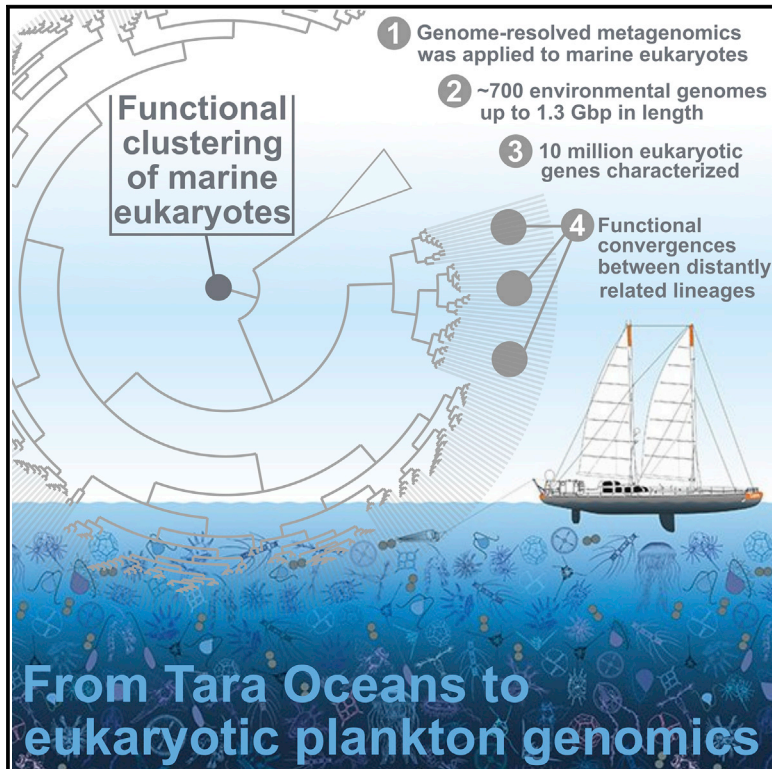


Functional repertoire convergence of distantly related eukaryotic plankton lineages abundant in the sunlit ocean

Graphical abstract



Authors

Tom O. Delmont, Morgan Gaia, Damien D. Hinsinger, ..., Eric Pelletier, Patrick Wincker, Olivier Jaillon

Correspondence

tom.delmont@genoscope.fr

In brief

Delmont et al. use nearly 300 billion metagenomic reads to characterize the genomic content of some of the most abundant and widespread eukaryotic populations in the sunlit ocean. This large genomic resource covers taxa underrepresented in our culture portfolio and exposes a functional convergence of distantly related eukaryotic plankton lineages.

Highlights

- Nearly 300 billion metagenomic reads were co-assembled from plankton in the oceans
- Hundreds of eukaryotic environmental genomes were characterized and curated
- These genomes better represent eukaryotic plankton compared to cultivation
- These genomes reveal a functional convergence of distantly related eukaryotes



Article

Functional repertoire convergence of distantly related eukaryotic plankton lineages abundant in the sunlit ocean

Tom O. Delmont,^{1,2,9,*} Morgan Gaia,^{1,2} Damien D. Hingsinger,^{1,2} Paul Frémont,^{1,2} Chiara Vanni,³ Antonio Fernandez-Guerra,⁴ A. Murat Eren,⁵ Artem Kourlaiev,^{1,2} Leo d'Agata,^{1,2} Quentin Clayssen,^{1,2} Emilie Villar,¹ Karine Labadie,^{1,2} Corinne Cruaud,^{1,2} Julie Poulain,^{1,2} Corinne Da Silva,^{1,2} Marc Wessner,^{1,2} Benjamin Noel,^{1,2} Jean-Marc Aury,^{1,2} Tara Oceans Coordinators, Colombar de Vargas,^{2,6} Chris Bowler,^{2,7} Eric Karsenti,^{2,6,8} Eric Pelletier,^{1,2} Patrick Wincker,^{1,2} and Olivier Jaillon^{1,2}

¹Génomique Métabolique, Genoscope, Institut François-Jacob, CEA, CNRS, Université d'Evry, Université Paris-Saclay, 91057 Evry, France

²Research Federation for the Study of Global Ocean Systems Ecology and Evolution, FR2022/Tara GOSEE, 75016 Paris, France

³Microbial Genomics and Bioinformatics Research Group, Max Planck Institute for Marine Microbiology, Bremen, Germany

⁴Lundbeck Foundation GeoGenetics Centre, GLOBE Institute, University of Copenhagen, Copenhagen, Denmark

⁵Helmholtz Institute for Functional Marine Biodiversity at Oldenburg, Germany

⁶Sorbonne Université and CNRS, UMR 7144 (AD2M), ECOMAP, Station Biologique de Roscoff, Roscoff, France

⁷Institut de Biologie de l'ENS, Département de Biologie, École Normale Supérieure, CNRS, INSERM, Université PSL, Paris, France

⁸Directors' Research, European Molecular Biology Laboratory, Heidelberg, Germany

⁹Lead contact

*Correspondence: tom.delmont@genoscope.fr

<https://doi.org/10.1016/j.xgen.2022.100123>

SUMMARY

Marine planktonic eukaryotes play critical roles in global biogeochemical cycles and climate. However, their poor representation in culture collections limits our understanding of the evolutionary history and genomic underpinnings of planktonic ecosystems. Here, we used 280 billion *Tara Oceans* metagenomic reads from polar, temperate, and tropical sunlit oceans to reconstruct and manually curate more than 700 abundant and widespread eukaryotic environmental genomes ranging from 10 Mbp to 1.3 Gbp. This genomic resource covers a wide range of poorly characterized eukaryotic lineages that complement long-standing contributions from culture collections while better representing plankton in the upper layer of the oceans. We performed the first, to our knowledge, comprehensive genome-wide functional classification of abundant unicellular eukaryotic plankton, revealing four major groups connecting distantly related lineages. Neither trophic modes of plankton nor its vertical evolutionary history could completely explain the functional repertoire convergence of major eukaryotic lineages that coexisted within oceanic currents for millions of years.

INTRODUCTION

Plankton in the sunlit ocean contribute about half of Earth's primary productivity, impacting global biogeochemical cycles and food webs.^{1,2} Plankton biomass appears to be dominated by unicellular eukaryotes and small animals^{3–6} including a phenomenal evolutionary and morphological biodiversity.^{5,7,8} The composition of planktonic communities is highly dynamical and shaped by biotic and abiotic variables, some of which are changing abnormally fast in the Anthropocene.^{9–11} Our understanding of marine eukaryotes has progressed substantially in recent years with the transcriptomic (e.g.,^{12,13}) and genomic (e.g.,^{14–16}) analyses of organisms isolated in culture and the emergence of efficient culture-independent surveys (e.g.,^{17,18}). However, most eukaryotic lineages' genomic content remains uncharacterized,^{19,20} limiting our understanding of their evolution, functioning, ecological interactions, and resilience to ongoing environmental changes.

Over the last decade, the *Tara Oceans* program has generated a homogeneous resource of marine plankton metagenomes and metatranscriptomes from the sunlit zone of all major oceans and two seas.²¹ Critically, most of the sequenced plankton size fractions correspond to eukaryotic organismal sizes, providing a prime dataset to survey genomic traits and expression patterns from this domain of life. More than 100 million eukaryotic gene clusters have been characterized by the metatranscriptomes, half of which have no similarity to known proteins.⁵ Most of them could not be linked to a genomic context,²² limiting their usefulness to gene-centric insights. The eukaryotic metagenomic dataset (the equivalent of ~10,000 human genomes) on the other hand has been partially used for plankton biogeographies,^{23,24} but it remains unexploited for the characterization of genes and genomes due to a lack of robust methodologies to make sense of its diversity.

Genome-resolved metagenomics²⁵ has been extensively applied to the smallest *Tara Oceans* plankton size fractions,



unveiling the ecology and evolution of thousands of viral, bacterial, and archaeal populations abundant in the sunlit ocean.^{26–31} This approach may thus be appropriate also to characterize the genomes of the most abundant eukaryotic plankton. However, very few eukaryotic genomes have been resolved from metagenomes thus far,^{26,32–35} in part due to their complexity (e.g., high density of repeats³⁶) and extended size³⁷ that might have convinced many of the unfeasibility of such a methodology. With the notable exception of some photosynthetic eukaryotes,^{26,32,35} metagenomics is lagging far behind cultivation for eukaryote genomics, contrasting with the two other domains of life. Here we fill this critical gap using hundreds of billions of metagenomic reads generated from the eukaryotic plankton size fractions of *Tara* Oceans and demonstrate that genome-resolved metagenomics is well suited for marine eukaryotic genomes of substantial complexity and length exceeding the emblematic gigabase. We used this new genomic resource to place major eukaryotic planktonic lineages in the tree of life and explore their evolutionary history based on both phylogenetic signals from conserved gene markers and present-day genomic functional landscape.

RESULTS AND DISCUSSION

A new resource of environmental genomes for eukaryotic plankton from the sunlit ocean

We performed the first, to our knowledge, comprehensive genome-resolved metagenomic survey of microbial eukaryotes from polar, temperate, and tropical sunlit oceans using 798 metagenomes (265 of which were released through the present study) derived from the *Tara* Oceans expeditions. They correspond to the surface and deep chlorophyll maximum layer of 143 stations from the Pacific, Atlantic, Indian, Arctic, and Southern Oceans, as well as the Mediterranean and Red Seas, encompassing eight eukaryote-enriched plankton size fractions ranging from 0.8 μm to 2 mm (Figure 1; Table S1). We used the 280 billion reads as inputs for 11 metagenomic co-assemblies (6–38 billion reads per co-assembly) using geographically bounded samples (Figure 1; Table S2), as previously done for the *Tara* Oceans 0.2–3 μm size fraction enriched in bacterial cells.²⁶ We favored co-assemblies to gain in coverage and optimize the recovery of large marine eukaryotic genomes. However, it is likely that other assembly strategies (e.g., from single samples) will provide access to genomic data our complex metagenomic co-assemblies failed to resolve. In addition, we used 158 eukaryotic single cells sorted by flow cytometry from seven *Tara* Oceans stations (Table S2) as input to perform complementary genomic assemblies (STAR Methods).

We thus created a culture-independent, non-redundant (average nucleotide identity <98%) genomic database for eukaryotic plankton in the sunlit ocean consisting of 683 metagenome-assembled genomes (MAGs) and 30 single-cell genomes (SAGs), all containing more than 10 million nucleotides (Table S3). These 713 MAGs and SAGs were manually characterized and curated using a holistic framework within *anvi'o*^{38,39} that relied heavily on differential coverage across metagenomes (STAR Methods and supplemental information). Nearly half the MAGs did not have vertical coverage >10 \times in any of the metagenomes, emphasizing the relevance of co-assemblies to gain

sufficient coverage for relatively large eukaryotic genomes. Moreover, one-third of the SAGs remained undetected by *Tara* Oceans' metagenomic reads, emphasizing cell sorting's power to target less abundant lineages. Absent from the MAGs and SAGs are DNA molecules physically associated with the focal eukaryotic populations, but that did not necessarily correlate with their nuclear genomes across metagenomes or had distinct sequence composition. They include chloroplasts, mitochondria, and viruses generally present in multi-copy. Finally, some highly conserved multi-copy genes such as the 18S rRNA gene were also missing due to technical issues associated with assembly and binning, following the fate of 16S rRNA genes in marine bacterial MAGs.²⁶

This new genomic database for eukaryotic plankton has a total size of 25.2 Gbp and contains 10,207,450 genes according to a workflow combining metatranscriptomics, *ab initio*, and protein-similarity approaches (STAR Methods). Estimated completion of the *Tara* Oceans MAGs and SAGs averaged to ~40% (redundancy of 0.5%) and ranged from 0.0% (a 15-Mbp-long Opisthokonta MAG) to 93.7% (a 47.8-Mbp-long Ascomycetes MAG). Genomic lengths averaged to 35.4 Mbp (up to 1.32 Gbp for the first giga-scale eukaryotic MAG, affiliated to *Odontella weissflogii*), with a GC-content ranging from 18.7% to 72.4% (Table S3). MAGs and SAGs are affiliated to Alveolata ($n = 44$), Amoebozoa ($n = 4$), Archaeplastida ($n = 64$), Cryptista ($n = 31$), Haptista ($n = 92$), Opisthokonta ($n = 299$), Rhizaria ($n = 2$), and Stramenopiles ($n = 174$). Only three closely related MAGs could not be affiliated to any known eukaryotic supergroup (see the phylogenetic section). Among the 713 MAGs and SAGs, 271 contained multiple genes corresponding to chlorophyll *a-b* binding proteins and were considered phytoplankton (Table S3). Genome-wide comparisons with 484 reference transcriptomes from isolates of marine eukaryotes (the METdb database⁴⁰ that improved data from MMETSP¹² and added new transcriptomes from *Tara* Oceans; see Table S3) linked only 24 of the MAGs and SAGs (~3%) to a eukaryotic population already in culture (average nucleotide identity >98%). These include well-known Archaeplastida populations within the genera *Micromonas*, *Bathycoccus*, *Ostreococcus*, *Pycnococcus*, *Chloropicon*, and *Prasinoderma* and a few taxa among Stramenopiles (e.g., the diatom *Minutocellus polymorphus*) and Haptista (e.g., *Phaeocystis cordata*). Among this limited number of matches, MAGs represented a nearly identical subset of the corresponding culture genomes (Figure S1, Table S4). Overall, we found metagenomics, single-cell genomics, and culture highly complementary with very few overlaps for marine eukaryotic plankton's genomic characterization.

The MAGs and SAGs recruited 39.1 billion reads with >90% identity (average identity of 97.4%) from 939 metagenomes, representing 11.8% of the *Tara* Oceans metagenomic dataset dedicated to unicellular and multicellular organisms ranging from 0.2 μm to 2 mm (Table S5). In contrast, METdb with a total size of ~23 Gbp recruited fewer than 7 billion reads (average identity of 97%), indicating that the collection of *Tara* Oceans MAGs and SAGs reported herein better represents the diversity of open ocean eukaryotes compared to transcriptomic data from decades of culture efforts worldwide. The majority of *Tara* Oceans metagenomic reads were still not recruited, which could be

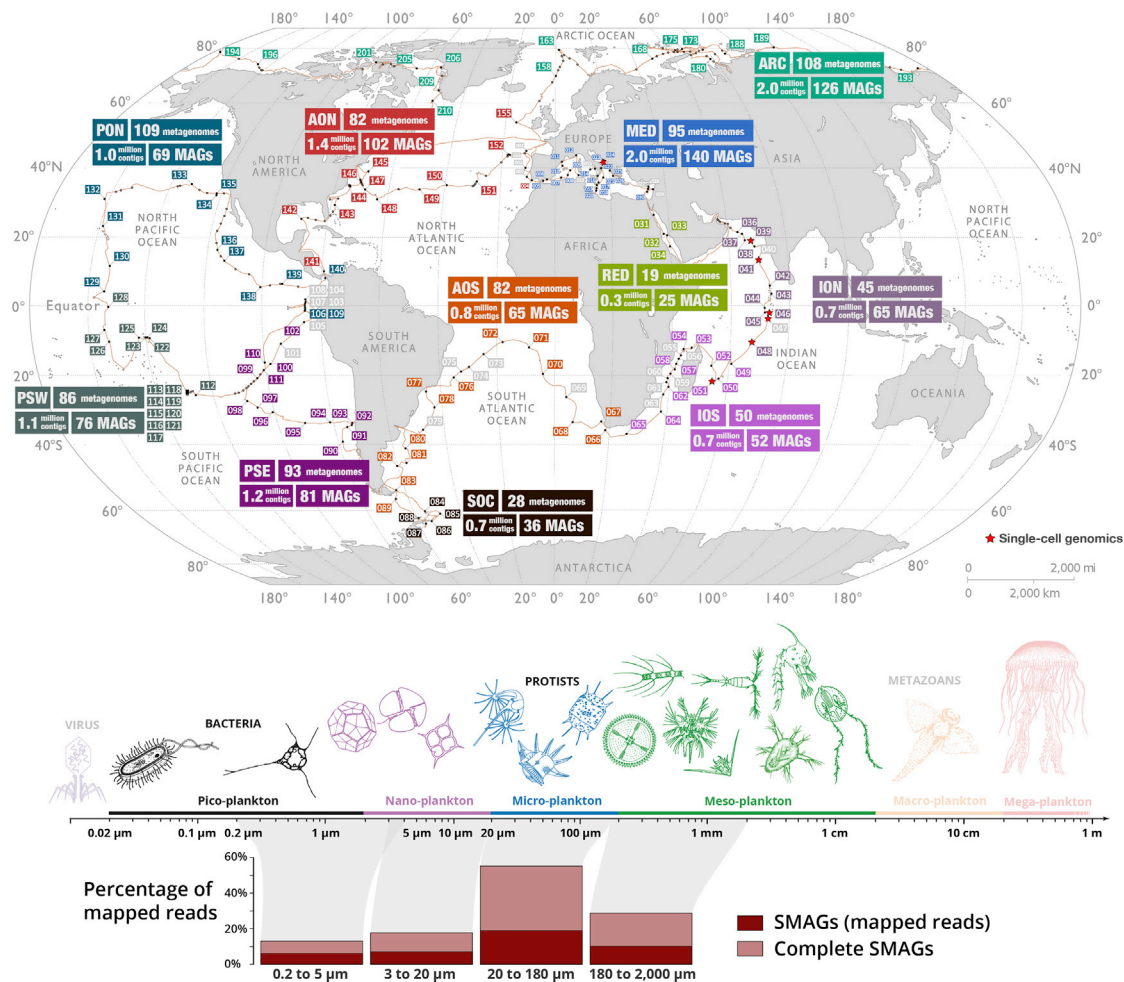


Figure 1. A genome-resolved metagenomic survey dedicated to eukaryotes in the sunlit ocean

The map displays Tara Oceans stations used to perform genome-resolved metagenomics, summarizes the number of metagenomes, contigs longer than 2,500 nucleotides, and eukaryotic MAGs characterized from each co-assembly, and outlines the stations used for single-cell genomics. ARC: Arctic Ocean; MED: Mediterranean Sea; RED: Red Sea; ION: Indian Ocean North; IOS: Indian Ocean South; SOC: Southern Ocean; AON: Atlantic Ocean North; AOS: Atlantic Ocean South; PON: Pacific Ocean North; PSE: Pacific South East; PSW: Pacific South West. The bottom panel summarizes mapping results from the MAGs and SAGs across 939 metagenomes organized into four size fractions. The mapping projection of complete MAGs and SAGs is described in the [STAR Methods](#) and [supplemental information](#).

explained by eukaryotic genomes that our methods failed to reconstruct, the occurrence of abundant bacterial, archaeal, and viral populations in the large size fractions we considered,^{41–43} and the incompleteness of the MAGs and SAGs. Indeed, with the assumption of correct completion estimates, complete MAGs and SAGs would have recruited ~26% of all metagenomic reads, including >50% of reads for the 20–180 μm size fraction alone due in part to an important contribution of hundreds of large copepod MAGs abundant within this cellular range (see [Figure 1](#) and [Table S5](#)).

Expanding the genomic representation of the eukaryotic tree of life

We then determined the phylogenetic distribution of the new ocean MAGs and SAGs in the tree of eukaryotic life. METdb was chosen as a taxonomically curated reference transcriptomic

database from culture collections, and the two largest subunits of the three DNA-dependent RNA polymerases (six multi-kilo-base genes found in all modern eukaryotes and hence already present in the last eukaryotic common ancestor) were selected. These genes are highly relevant markers for the phylogenetic inference of distantly related microbial organisms⁴⁴ and contributed to our understanding of eukaryogenesis.⁴⁵ They have long been overlooked to study the eukaryotic tree of life, possibly because automatic methods are currently missing to effectively identify each DNA-dependent RNA polymerase type prior to performing the phylogenetic analyses. Here, protein sequences were identified using hidden markov models (HMMs) dedicated to the two largest subunits for the MAGs and SAGs (n = 2,150) and METdb reference transcriptomes (n = 2,032). These proteins were manually curated and linked to the corresponding DNA-dependent RNA polymerase types for each subunit using

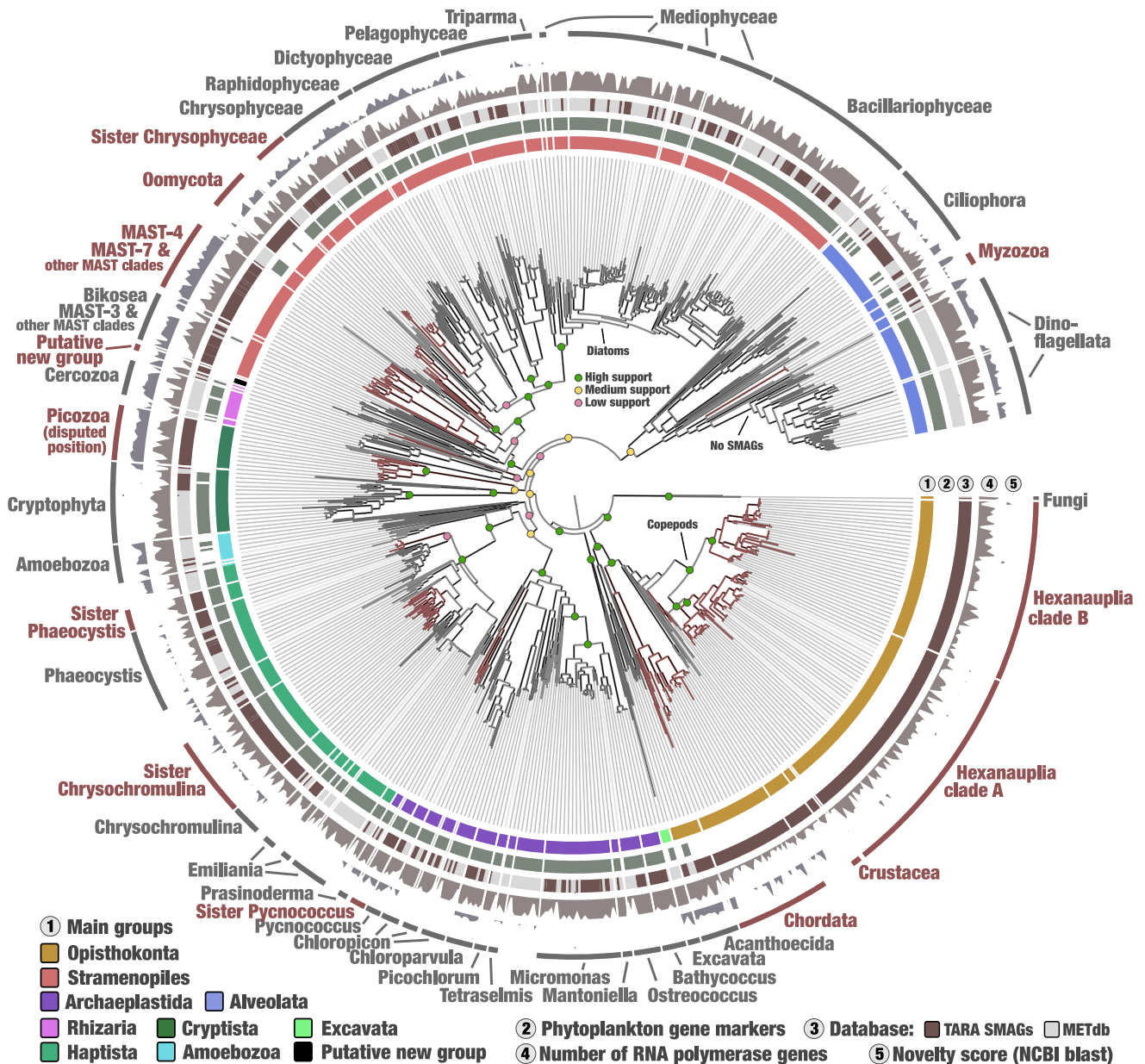


Figure 2. Phylogenetic analysis of concatenated DNA-dependent RNA polymerase protein sequences from eukaryotic plankton

The maximum-likelihood phylogenetic tree of the concatenated two largest subunits from the three DNA-dependent RNA polymerases (six genes in total) included Tara Oceans MAGs and SAGs and METdb transcriptomes and was generated using a total of 7,243 sites in the alignment and LG + F + R10 model; Opisthokonta was used as the outgroup. Supports for selected clades are displayed. Phylogenetic supports were considered high (aLRT \geq 80 and UFBoot \geq 95), medium (aLRT \geq 80 or UFBoot \geq 95), or low (aLRT $<$ 80 and UFBoot $<$ 95) (STAR Methods). The tree was decorated with additional layers using the anvio interface. The novelty score layer (STAR Methods) was set with a minimum of 30 (i.e., 70% similarity) and a maximum of 60 (i.e., 40% similarity). Branches and names in red correspond to main lineages lacking representatives in METdb.

reference proteins and phylogenetic inferences (STAR Methods and supplemental information). BLAST results provided a novelty score for each of them (STAR Methods and Table S3), expanding the scope of our analysis to eukaryotic genomes stored in NCBI as of August 2020. Our final phylogenetic analysis included 416 reference transcriptomes and 576 environmental MAGs and SAGs that contained at least one of the six marker

genes (Figure 2). The concatenated DNA-dependent RNA polymerase protein sequences effectively reconstructed a coherent tree of eukaryotic life, comparable to previous large-scale phylogenetic analyses based on other gene markers,⁴⁶ and to a complementary BUSCO-centric phylogenomic analysis using protein sequences corresponding to hundreds of smaller gene markers (Figure S2). As a noticeable difference, the Haptista

were most closely related to Archaeplastida, while Cryptista included the phylum Picozoa and was most closely related to the TSAR supergroup (Telonemia not represented here, Stramenopiles, Alveolata, and Rhizaria), albeit with weaker supports. This view of the eukaryotic tree of life using a previously under-exploited universal marker is by no means conclusive by itself but contributes to ongoing efforts to understand deep evolutionary relationships among eukaryotes while providing an effective framework to assess the phylogenetic positions of a large number of the *Tara* Oceans MAGs and SAGs.

Among small planktonic animals, the *Tara* Oceans MAGs recovered one lineage of Chordata related to the Oikopleuridae family, and Crustacea including a wide range of copepods (Figure 2; Table S3). Copepods dominate large size fractions of plankton⁸ and represent some of the most abundant animals on the planet.^{47,48} They actively feed on unicellular plankton and are a significant food source for larger animals such as fish, thus representing a key trophic link within the global carbon cycle.⁴⁹ For now, fewer than ten copepod genomes have been characterized by isolates.^{50,51} The additional 8.4 Gbp of genomic material unveiled herein is split into 217 MAGs, and themselves organized into two main phylogenetic clusters that we dubbed marine Hexanauplia clades A and B. The two clades considerably expanded the known genomic diversity of copepods, albeit clade B was linked to few reference genomes (Figure S3). These clades were equally abundant and detected in all oceanic regions. Copepod MAGs typically had broad geographic distributions, being detected on average in 25% of the globally distributed *Tara* Oceans stations. In comparison, Opisthokonta MAGs affiliated to Chordata and Choanoflagellata (Acanthoecida) were, on average, detected in less than 10% of sampling sites.

Generally occurring in smaller size fractions, MAGs and SAGs corresponding to unicellular eukaryotes considerably expanded our genomic knowledge of known genera within Alveolata, Archaeplastida, Haptista, and Stramenopiles (Figure 2; Table S3). Just within the diatoms for instance (Stramenopiles), MAGs were reconstructed for *Fragilariopsis* (n = 5), *Pseudo-nitzschia* (n = 7), *Chaetoceros* (n = 11), *Thalassiosira* (n = 5), and seven other genera (including the intriguing >1-Gbp-long genome of a blooming *O. weissflogii* species), all of which are known to contribute significantly to photosynthesis in the sunlit ocean.^{52,53} Among the Archaeplastida, genome-wide average nucleotide identities and distribution patterns indicated that the large majority of MAGs correspond to distinct populations, many of which have not been characterized by means of culture genomics. Especially, we characterized the genomic content of at least 16 *Micromonas* populations (Figure S4), 11 *Chloropicon* populations (Figure S5), and five *Bathycoccus* populations (Figure S6). Beyond this genomic expansion of known planktonic genera, MAGs and SAGs covered various lineages lacking representatives in METdb. These included (1) Picozoa as a sister clade to Cryptista (SAGs from this phylum were recently linked to the Archaeplastida using different gene markers and databases⁵⁴), to the class Chrysophyceae, and the genera *Phaeocystis* and *Pycnococcus*, (2) basal lineages of Oomycota within Stramenopiles and Myzozoa within Alveolata, (3) multiple branches within the MAST lineages⁵⁵ (Figure S7), (4) and a small cluster possibly

at the root of Rhizaria we dubbed “putative new group” (Figure S8). The novelty score of individual DNA-dependent RNA polymerase genes was supportive of the topology of the tree. Significantly, diverse MAST lineages, Picozoa, and the putative new group all displayed a deep branching distance from cultures and a high novelty score. In addition, the BUSCO-centric phylogenomic analysis placed the “putative new group” at the root of Haptista (Figure S2), supporting its high novelty while stressing the difficulty placing it accurately in the eukaryotic tree of life. In addition, this alternative phylogenomic analysis confirmed placement for the sister clade to *Phaeocystis* but not for the sister clade to *Pycnococcus*, placing it instead as a stand-alone lineage distinct from any Archaeplastida lineages represented by the MAGs, SAGs, and METdb. While different gene markers might provide slightly different evolutionary trends, a well-known phylogenetic phenomenon, here our two approaches concur when it comes to emphasizing the genomic novelty of the MAGs and SAGs compared with culture references.

One of the most conspicuous lineages lacking any MAGs and SAGs was the Dinoflagellata, a prominent and extremely diverse phylum in small and large eukaryotic size fractions of *Tara* Oceans.⁸ These organisms harbor very large and complex genomes⁵⁶ that likely require much deeper sequencing efforts to be recovered by genome-resolved metagenomics. Besides, many other important lineages are also missing in MAGs and SAGs (e.g., within Radiolaria and Excavata), possibly due to a lack of abundant populations despite their diversity.

A complex interplay between the evolution and functioning of marine eukaryotes

MAGs and SAGs provided a broad genomic assessment of the eukaryotic tree of life within the sunlit ocean by covering a wide range of marine plankton eukaryotes distantly related to cultures but abundant in the open ocean. Thus, the resource provided an opportunity to explore the interplay between the phylogenetic signal and functional repertoire of eukaryotic plankton with genomics. With EggNOG,^{57–59} we identified orthologous groups corresponding to known (n = 15,870) and unknown functions (n = 12,567), orthologous groups with no assigned function at <http://eggnog5.embl.de/> for 4.7 million genes (nearly 50% of the genes; STAR Methods). Among them, functional redundancy (i.e., a function detected multiple times in the same MAG or SAG) encompassed 46.6%–96.8% of the gene repertoires (average of 75.2% of functionally redundant genes). We then used these gene annotations to classify the MAGs and SAGs based on their functional profiles (Table S6). Our hierarchical clustering analysis using Euclidean distance and Ward linkage (an approach to organize genomes based on pangenomic traits⁶⁰) first split the MAGs and SAGs into small animals (Chordata, Crustacea, copepods) and putative unicellular eukaryotes (Figure 3). Fine-grained functional clusters exhibited a highly coherent taxonomy within the unicellular eukaryotes. For instance, MAGs affiliated to the coccolithophore *Emiliana* (completion ranging from 7.8% to 32.2%), Dictyochophyceae family (completion ranging from 8.6% to 76.9%), and the sister clade to *Phaeocystis* (completion ranging from 18.4% to 60.4%) formed distinct clusters. The phylum Picozoa (completion ranging from 1.6% to 75.7%) was also confined to a single cluster that could be explained partly

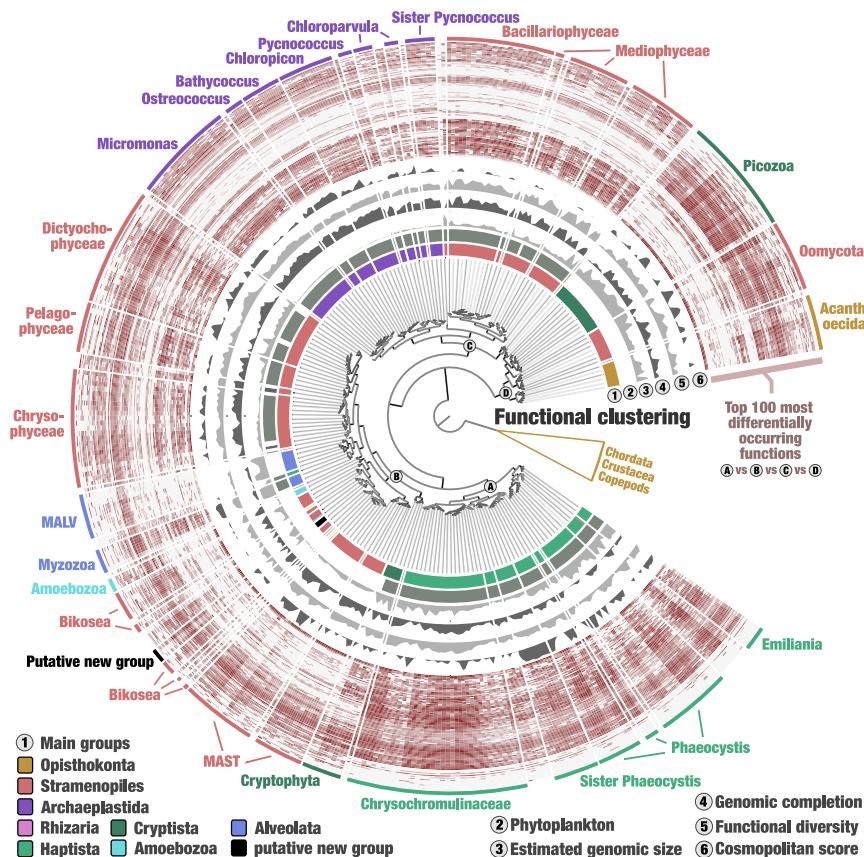


Figure 3. The genomic functional landscape of unicellular eukaryotes in the sunlit ocean

The figure displays a hierarchical clustering (Euclidean distance with Ward's linkage) of 681 MAGs and SAGs based on the occurrence of ~28,000 functions identified with EggNOG^{57–59}, rooted with small animals (Chordata, Crustacea, and copepods) and decorated with layers of information using the anvio interactive interface. Layers include the occurrence in log₁₀ of 100 functions with lowest p value when performing Welch's ANOVA between the functional groups A, B, C and D (see nodes in the tree). Removed from the analysis were Ciliophora MAGs (gene calling is problematic for this lineage), two less complete MAGs affiliated to Opisthokonta, and functions occurring more than 500 times in the gigabase-scale MAG and linked to retrotransposons connecting otherwise unrelated MAGs and SAGs.

by a considerable radiation of genes related to dioxygenase activity (up to 644 genes). Most strikingly, the Archaeplastida MAGs not only clustered with respect to their genus-level taxonomy, but the organization of these clusters was highly coherent with their evolutionary relationships (see Figure 2), confirming not only the novelty of the putative sister clade to *Pycnococcus*, but also the sensitivity of our framework to draw the functional landscape of unicellular marine eukaryotes. Clearly, the important functional redundancy of MAGs and SAGs minimized the effect of genomic incompleteness in our efforts assessing the functional profile of unicellular marine eukaryotes.

Four major functional groups of unicellular eukaryotes emerged from the hierarchical clustering (Figure 3), which was perfectly recapitulated when incorporating the standard culture genomes matching to a MAG (Figure S9) and when clustering only the MAGs and SAGs >25% complete (Figure S10). Importantly, the taxonomic coherence observed in fine-grained clusters vanished when moving toward the root of these functional groups. Group A was an exception since it only covered the Haptista (including the highly cosmopolitan sister clade to *Phaeocystis*). Group B, on the other hand, encompassed a highly diverse and polyphyletic group of distantly related heterotrophic (e.g., MAST and MALV) and mixotrophic (e.g., Myzozoa and Cryptophyta) lineages of various genomic size, suggesting that broad genomic functional trends may not only be explained by the trophic mode of plankton. Group C was mostly photosynthetic and covered the diatoms (Stramenopiles of various genomic size)

and Archaeplastida (small genomes) as sister clusters. This finding likely reflects that diatoms are the only group with an obligatory photoautotrophic lifestyle within the Stramenopiles, like the Archaeplastida. Finally, Group D encompassed three distantly related lineages of heterotrophs (those systematically lacked gene markers for photosynthesis) exhibiting rather large genomes: Oomycota, Acanthoecida choanoflagellates, and Picozoa. Those four functional groups have similar amounts of detected functions and contained both cosmopolite and rarely detected MAGs and SAGs across the *Tara* Oceans stations. While attempts to classify marine eukaryotes based on genomic functional traits have been made in the past (e.g., using a few SAGs⁶¹), our resource therefore provided a broad enough spectrum of genomic material for a first genome-wide functional classification of abundant lineages of unicellular eukaryotic plankton in the upper layer of the ocean.

A total of 2,588 known and 680 unknown functions covering 1.94 million genes (~40% of the annotated genes) were significantly differentially occurring between the four functional groups (Welch's ANOVA tests, p value < 1.e⁻⁰⁵; Table S6). We displayed the occurrence of the 100 functions with lowest p values in the hierarchical clustering presented in Figure 3 to illustrate and help convey the strong signal between groups. However, more than 3,000 functions contributed to the basic partitioning of MAGs and SAGs. They cover all high-level functional categories identified in the 4.7 million genes with similar proportions (Figure S11), indicating that a wide range of functions related to information storage and processing, cellular processes and signaling, and metabolism contribute to the partitioning of the groups. As a notable difference, functions related to transcription (-50%) and RNA processing and modification (-47%) were less represented, while those related to carbohydrate transport and metabolism were enriched (+43%) in the

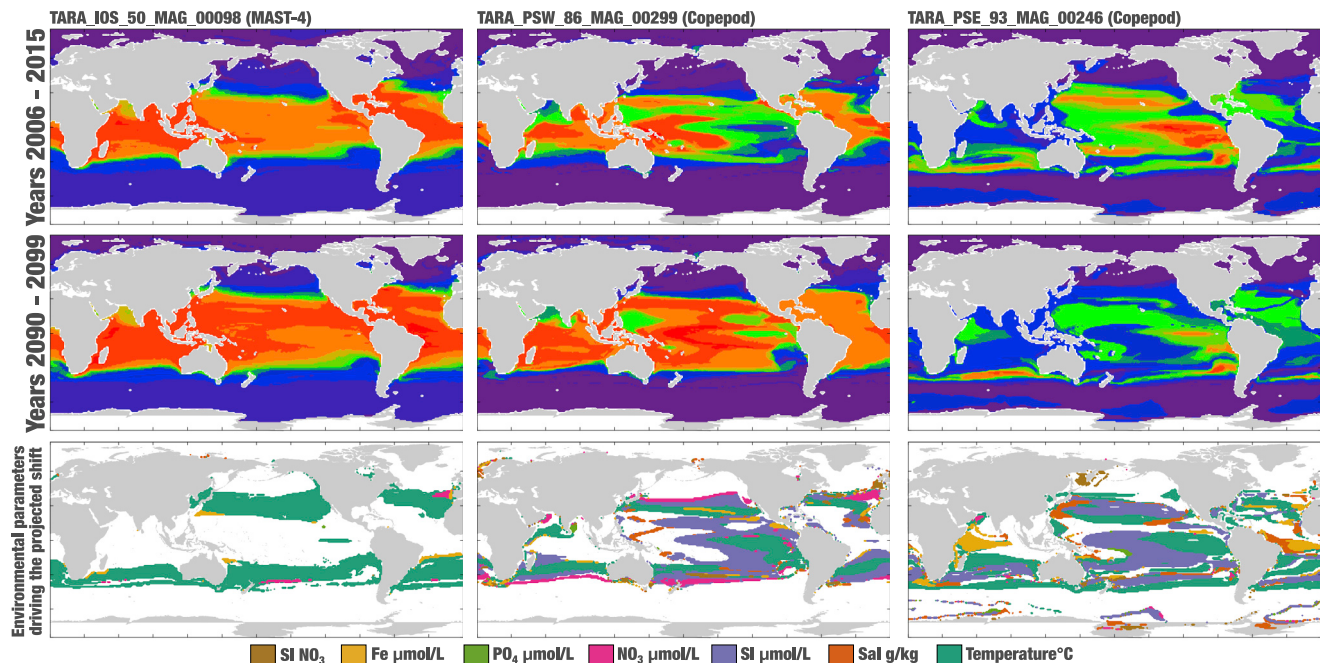


Figure 4. World map distribution projections for three eukaryotic MAGs during the periods of 2006–15 and 2090–99

The probability of presence ranges from 0 (purple) to 1 (red), with green corresponding to a probability of 0.5. The bottom row displays first-rank region-dependent environmental parameters driving the projected shifts of distribution (in regions where $|\Delta P| > 0.1$). Noticeably, projected decreases of silicate in equatorial regions drive 34% of the expansion of TARA_PSW_MAG_00,299 while driving 34% of the reduction of TARA_PSE_93_MAG_00,246, possibly reflecting different life strategies of these copepods (e.g., grazing). In contrast, the expansion of TARA_IOS_50_MAG_00,098 is mostly driven by temperature (74%).

differentially occurring functions. Interestingly, we noticed within Group C a scarcity of various functions otherwise occurring in high abundance among unicellular eukaryotes. These included functions related to ion channels (e.g., extracellular ligand-gated ion channel activity, intracellular chloride channel activity, magnesium ion transmembrane transporter activity, calcium ion transmembrane transport, calcium sodium antiporter activity) that may be linked to flagellar motility and the response to external stimuli,⁶² reflecting the lifestyle of true autotrophs. Group D, on the other hand, had significant enrichment of various functions associated with carbohydrate transport and metabolism (e.g., alpha and beta-galactosidase activities, glycosyl hydrolase families, glycogen debranching enzyme, alpha-L-fucosidase), denoting a distinct carbon acquisition strategy. Overall, the properties of thousands of differentially occurring functions suggest that eukaryotic plankton's complex functional diversity is vastly intertwined within the tree of life, as inferred from phylogenies. This reflects the complex nature of the genomic structure and phenotypic evolution of organisms, which rarely fit their evolutionary relationships.

To this point, our analysis focused on the 4.4 million genes that were functionally annotated to EggNOG, which discarded more than half of the genes we identified in the MAGs and SAGs. Our current lack of understanding of many eukaryotic functional genes even within the scope of model organisms⁶³ can explain the limits of reference-based approaches to study the gene content of eukaryotic plankton. Thus, to gain further insights and overcome these limitations, we partitioned and categorized the eukaryotic gene content with AGNOSTOS.⁶⁴ AGNOSTOS

grouped 5.4 million genes in 424,837 groups of genes sharing remote homologies, adding 2.3 million genes left uncharacterized by the EggNOG annotation. AGNOSTOS applies a strict set of parameters for the grouping of genes discarding 575,053 genes by its quality controls and 4,264,489 genes in singletons. The integration of the EggNOG annotations into AGNOSTOS resulted in a combined dataset of 25,703 EggNOG orthologous groups (singletons and gene clusters) and 271,464 AGNOSTOS groups of genes, encompassing 6.4 million genes, 45% more genes than the original dataset (STAR Methods). The genome-wide functional classification of MAGs and SAGs based on this extended set of genes supported most trends previously observed with EggNOG annotation alone (Figure S12; Table S7), reinforcing our observations. But most interestingly, classification based solely on 23,674 newly identified groups of genes of unknown function (Table S8; a total of 1.3 million genes discarded by EggNOG) were also supportive of the overall trends, including notable links between diatoms and green algae and between Picozoa and Acanthoecida (Figure S13). Thus, we identified a functional repertoire convergence of distantly related eukaryotic plankton lineages in both the known and unknown coding sequence space, the latter representing a substantial amount of biologically relevant gene diversity.

Niche and biogeography of individual eukaryotic populations

Besides insights into organismal evolution and genomic functions, the MAGs and SAGs provided an opportunity to evaluate

the present and future geographical distribution of eukaryotic planktonic populations (close to species-level resolution) using the genome-wide metagenomic read recruitments. Here, we determined the niche characteristics (e.g., temperature range) of 374 MAGs and SAGs (~50% of the resource) detected in at least five stations (Table S9) and used climate models to project world map distributions (http://end.mio.osupytheas.fr/Ecological_Niche_database/) based on climatologies for the periods of 2006–15 and 2090–99²⁴ (STAR Methods and supplemental information).

Each of these MAGs and SAGs was estimated to occur in a surface averaging 42 and 39 million km² for the first and second period, respectively, corresponding to ~12% of the surface of the ocean. Our data suggest that most eukaryotic populations in the database will remain widespread for decades to come. However, many changes in biogeography are projected to occur. For instance, the most widespread population in the first period (a MAST MAG) would still be ranked first at the end of the century but with a surface area increasing from 37% to 46% (Figure 4), a gain of 28 million km² corresponding to the surface of North America. Its expansion from the tropics toward more temperate oceanic regions regardless of longitude is mostly explained by temperature and reflects the expansion of tropical niches due to global warming, echoing recent predictions made with amplicon surveys and imaging data.⁶⁵ As an extreme case, the MAG benefiting the most between the two periods (a copepod) could experience a gain of 55 million km² (Figure 4), more than the surface of Asia and Europe combined. On the other hand, the MAG losing most ground (also a copepod) could undergo a decrease of 47 million km². Projected changes in these two examples correlated with various variables (including a notable contribution of silicate), an important reminder that temperature alone cannot explain plankton's biogeography in the ocean. Our integration of genomics, metagenomics, and climate models provided the resolution needed to project individual eukaryotic population niche trajectories in the sunlit ocean.

Limitations of the study

Genome-resolved metagenomics applied to the considerable environmental DNA sequencing legacy of the *Tara* Oceans large cellular size fractions proved effective at complementing our culture portfolio of marine eukaryotes. Nevertheless, the approach failed to cover lineages (1) containing very large genomes (e.g., the Dinoflagelates⁵⁶), (2) only found in low abundance, (3) or found to be abundant but with unusually high levels of microdiversity, challenging metagenomic assemblies (e.g., the prominent *Pelagomonas* genus⁵⁶ for which we only recovered high latitude MAG representatives). Deeper sequencing efforts coupled with long read sequencing technologies will likely overcome many of these limitations in years to come.

Our functional clustering of marine eukaryotes took advantage of a wide range of genomes manually characterized with the platform *anvi'o*, and also considered numerous gene clusters of unknown function using the AGNOSTOS framework. However, this methodology also contains noticeable limitations. For instance, clustering methodologies can influence the observed trends. Furthermore, integration of additional taxonomic groups that

currently lack genomic characterizations might impact functional clustering, similar to what is often observed with phylogenomic analyses. Thus, we anticipate that follow-up investigations might identify functional clusters slightly differing from the four major groups we have identified, refining our understanding of the functional convergence of distantly related eukaryotic lineages identified in our study.

CONCLUSION

Similar to recent advances that elucidated viral, bacterial, and archaeal lineages, microbiology is experiencing a shift from cultivation to metagenomics for the genomic characterization of marine eukaryotes *en masse*. Indeed, our culture-independent and manually curated genomic characterization of abundant unicellular eukaryotic populations and microscopic animals in the sunlit ocean covers a wide range of poorly characterized lineages from multiple trophic levels (e.g., copepods and their prey, mixotrophs, autotrophs, and parasites) and provided the first gigabase-scale metagenome-assembled genome. Our genome-resolved survey and parallel efforts by others^{67,68} are not only different from past transcriptomic surveys of isolated marine organisms but also better represent eukaryotic plankton in the open photic ocean. They represent innovative steps toward using genomics to explore in concert the ecological and evolutionary underpinnings of environmentally relevant eukaryotic organisms, using metagenomics to fill critical gaps in our remarkable culture portfolio.²¹

Phylogenetic gene markers such as the DNA-dependent RNA polymerases (the basis of our phylogenetic analysis) provide a critical understanding of the origin of eukaryotic lineages and allowed us to place most environmental genomes in a comprehensible evolutionary framework. However, this framework is based on sequence variations within core genes that in theory are inherited from the last eukaryotic common ancestor representing the vertical evolution of eukaryotes, disconnected from the structure of genomes. As such, it does not recapitulate the functional evolutionary journey of plankton, as demonstrated in our genome-wide functional classification of unicellular eukaryotes in both the known and unknown coding sequence space. The dichotomy between phylogeny and function was already well described with morphological and other phenotypic traits and could be explained in part by secondary endosymbiosis events that have spread plastids and genes for their photosynthetic capabilities across the eukaryotic tree of life.^{69–72} Here we moved beyond morphological inferences and disentangled the phylogeny of gene markers and broad genomic functional repertoire of a comprehensive collection of marine eukaryotic lineages. We identified four major genomic functional groups of unicellular eukaryotes made of distantly related lineages. The Stramenopiles proved particularly effective in terms of genomic functional diversification, possibly explaining part of their remarkable success in this biome.^{8,73}

The topology of phylogenetic trees compared to the functional clustering of a wide range of eukaryotic lineages has revealed contrasting evolutionary journeys for widely scrutinized gene markers of evolution and less studied genomic functions of plankton. The apparent functional convergence of distantly

related lineages that coexisted in the same biome for millions of years could not be explained by either a vertical evolutionary history of unicellular eukaryotes nor their trophic modes (phytoplankton versus heterotrophs), shedding new lights into the complex functional dynamics of plankton over evolutionary time scales. Convergent evolution is a well-known phenomenon of independent origin of biological traits such as molecules and behaviors^{74,75} that has been observed in the morphology of microbial eukaryotes⁷⁶ and is often driven by common selective pressures within similar environmental conditions. However, an independent origin of similar functional profiles is not the only possible explanation for organisms sharing the same habitat. Indeed, one could wonder if lateral gene transfers between eukaryotes^{77,78} have played a central role in these processes, as previously observed between eukaryotic plant pathogens⁷⁹ or grasses.⁸⁰ As a case in point, secondary endosymbiosis events are known to have resulted in massive gene transfers between endosymbionts and their hosts in the oceans.^{69,70} In particular, these events involved transfers of genes from green algae to diatoms,⁸¹ two lineages clustering together in our genomic functional classification of eukaryotic plankton. However, lineages sharing the same secondary endosymbiotic history did not always fall in the same functional group. This was the case for diatoms, Haptista, and Cryptista that have different functional trends yet originate from a common ancestor that likely acquired its plastid from red and green algae.^{69,70,82} Surveying phylogenetic trends for functions derived from the ~10 million genes identified here will likely contribute to new insights regarding the extent of lateral gene transfers between eukaryotes,^{83,84} the independent emergence of functional traits (convergent evolution), as well as functional losses between lineages,⁸⁵ that altogether might have driven the functional convergences of distantly related eukaryotic lineages abundant in the sunlit ocean.

Regardless of the mechanisms involved, the functional repertoire convergences we observed likely highlight primary organismal functioning, which have fundamental impacts on plankton ecology, and their functions within marine ecosystems and biogeochemical cycles. Thus, the apparent dichotomy between phylogenies (a vertical evolutionary framework) and genome-wide functional repertoires (genome structure evolution) depicted here should be viewed as a fundamental attribute of marine unicellular eukaryotes that we suggest warrants a new rationale for studying the structure and state of plankton, a rationale also based on present-day genomic functions rather than phylogenetic and morphological surveys alone.

CONSORTIA

Shinichi Sunagawa, Silvia G. Acinas, Peer Bork, Eric Karsenti, Chris Bowler, Christian Sardet, Lars Stemmann, Coloman de Vargas, Patrick Wincker, Magali Lescot, Marcel Babin, Gabriel Gorsky, Nigel Grimsley, Lionel Guidi, Pascal Hingamp, Olivier Jaillon, Stefanie Kandels, Daniele Iudicone, Hiroyuki Ogata, Stéphane Pesant, Matthew B. Sullivan, Fabrice Not, Lee Karp-Boss, Emmanuel Boss, Guy Cochrane, Michael Follows, Nicole Poulton, Jeroen Raes, Mike Sieracki, and Sabrina Speich.

STAR★METHODS

Detailed methods are provided in the online version of this paper and include the following:

- **KEY RESOURCES TABLE**
- **RESOURCE AVAILABILITY**
 - Lead contact
 - Materials availability
 - Data and code availability
- **METHOD DETAILS**
 - *Tara* Oceans metagenomes
 - Genome-resolved metagenomics
 - A first gigabase scale eukaryotic MAG
 - MAGs from the 0.2–3 μm size fraction
 - Single-cell genomics
 - Characterization of a non-redundant database of MAGs and SAGs
 - Taxonomical inference of MAGs and SAGs
 - Protein coding genes
 - Protein-coding genes for the MAGs
 - Protein coding genes for the SAGs
 - BUSCO completion scores for protein-coding genes in MAGs and SAGs
 - Biogeography of MAGs and SAGs
 - Identifying the environmental niche of MAGs and SAGs
 - Cosmopolitan score
 - A database of manually curated DNA-dependent RNA polymerase genes
 - Novelty score for the DNA-dependent RNA polymerase genes
 - Phylogenetic analyses of MAGs and SAGs
 - EggNOG functional inference of MAGs and SAGs
 - Eukaryotic MAGs and SAGs integration in the AGNOSTOS-DB
 - AGNOSTOS functional aggregation inference
 - Functional clustering of MAGs and SAGs
- **QUANTIFICATION AND STATISTICAL ANALYSIS**
 - Differential occurrence of functions

SUPPLEMENTAL INFORMATION

Supplemental information can be found online at <https://doi.org/10.1016/j.xgen.2022.100123>.

ACKNOWLEDGMENTS

Our survey was made possible by two scientific endeavors: the sampling and sequencing efforts by the *Tara* Oceans Project and the bioinformatics and visualization capabilities afforded by *anvi'o*. We are indebted to all who contributed to these efforts, as well as other open-source bioinformatics tools for their commitment to transparency and openness. *Tara* Oceans (which includes the *Tara* Oceans and *Tara* Oceans Polar Circle expeditions) would not exist without the leadership of the *Tara* Ocean Foundation and the continuous support of 23 institutes (<https://oceans.taraexpeditions.org/>). We thank the commitment of the following people and sponsors who made this singular expedition possible: CNRS (in particular Groupement de Recherche GDR3280 and the Research Federation for the Study of Global Ocean Systems Ecology and Evolution FR2022/Tara GOSEE), the European Molecular Biology Laboratory (EMBL), Genoscope/CEA, the French Ministry of Research and the French Government 'Investissement d'Avenir'

programs Oceanomics (ANR-11-BTBR-0008), FRANCE GENOMIQUE (ANR-10-INBS-09), ATIGE Genopole postdoctoral fellowship, HYDROGEN/ANR-14-CE23-0001, MEMO LIFE (ANR-10-LABX-54), PSL Research University (ANR-11-IDEX-0001-02) and EMBRC-France (ANR-10-INBS-02), Fund for Scientific Research—Flanders, VIB, Stazione Zoologica Anton Dohrn, UNIMIB, ANR (projects ALGALVIRUS ANR-17-CE02-0012, PHYTBAC/ANR-2010-1709-01, POSEIDON/ANR-09-BLAN-0348, PROMETHEUS/ANR-09-PCS-GENM-217, TARA-GIRUS/ANR-09-PCS-GENM-218), EU FP7 (MicroB3/No. 287589, IHMS/HEALTH-F4-2010-261376), Genopole, CEA DRF Impulsion program, OCEANOMICS (project no. ANR-11-BTBR-0008), ERC Advanced Award Diatomic (grant agreement No 835067) to CB. The authors also thank Agnès B. and E. Bourgois, the Prince Albert II de Monaco Foundation, the Veolia Foundation, the EDF Foundation, Region Bretagne, Lorient Agglomération, Worldcourier, Illumina, Serge Ferrari, and the Fonds Français pour l'Environnement Mondial for support and commitment. The global sampling effort was made possible by countless scientists and crew who performed sampling aboard the *Tara* from 2009 to 2013. The authors are also grateful to the countries that graciously granted sampling permission. Part of the computations were performed using the platine, titane, and curie HPC machine provided through GENCI grants (t2011076389, t2012076389, t2013036389, t2014036389, t2015036389, and t2016036389). We also thank Noan Le Bescot (TernogDesign) for artwork on figures.

AUTHOR CONTRIBUTIONS

D.D.H., M.G., E.P., P.W., O.J., and T.O.D. conducted the study. T.O.D. and M.G. characterized the MAGs and SAGs, and RNA polymerase genes, respectively. D.D.H. (analysis of the ~10 million genes), M.G. (phylogenies), P.F. (climate models and world map projections), E.P. (METdb database, mapping results), and T.O.D. performed the primary analysis of the data. A.K., L.d.A., Q.C., and J.-M.A. assembled and annotated the single cell genomes and helped to process metagenomic assemblies. E.V., M.W., B.N., C.D.S., D.D.H., O.J., and J.-M.A. identified the eukaryotic genes in the MAG assemblies. A.F.G. and C.V. characterized the repertoire of functions in the unknown coding sequence space. T.O.D. wrote the manuscript with critical inputs from all the authors. This article is contribution number 132 of *Tara Oceans*.

DECLARATION OF INTERESTS

The authors declare no competing interests.

Received: February 16, 2021

Revised: December 10, 2021

Accepted: April 4, 2022

Published: April 28, 2022

REFERENCES

- Boyd, P.W. (2015). Toward quantifying the response of the oceans' biological pump to climate change. *Front. Mar. Sci.* *2*, 77.
- Sanders, R., Henson, S.A., Koski, M., De La Rocha, C.L., Painter, S.C., Poulton, A.J., Riley, J., Salihoglu, B., Visser, A., Yool, A., et al. (2014). The biological carbon pump in the North Atlantic. *Prog. Oceanogr.* *129*, 200–218.
- Dortch, Q., and Packard, T.T. (1989). Differences in biomass structure between oligotrophic and eutrophic marine ecosystems. *Deep Sea Res. Part. A. Oceanogr. Res. Pap.* *36*, 223–240.
- Gasol, J.M., Del Giorgio, P.A., and Duarte, C.M. (1997). Biomass distribution in marine planktonic communities. *Limnol. Oceanogr.* *42*, 1353–1363.
- Carradec, Q., Pelletier, E., Da Silva, C., Alberti, A., Seeleuthner, Y., Blanchet, R., Lima-Mendez, G., Rocha, F., Tirichine, L., Labadie, K., et al. (2018). A global ocean atlas of eukaryotic genes. *Nat. Commun.* *9*, 1–13.
- Caron, D.A., Countway, P.D., Jones, A.C., Kim, D.Y., and Schnetzer, A. (2011). Marine protistan diversity. *Ann. Rev. Mar. Sci.* *4*, 467–493.
- Leray, M., and Knowlton, N. (2016). Censusing marine eukaryotic diversity in the twenty-first century. *Philos. Trans. R. Soc. B Biol. Sci.* *371*, 20150331.
- De Vargas, C., Audic, S., Henry, N., Decelle, J., Mahé, F., Logares, R., Lara, E., Berney, C., Le Bescot, N., Probert, I., et al. (2015). Eukaryotic plankton diversity in the sunlit ocean. *Science* *348*, 1261605.
- Jonkers, L., Hillebrand, H., and Kucera, M. (2019). Global change drives modern plankton communities away from the pre-industrial state. *Nature* *570*, 372–375.
- Hays, G.C., Richardson, A.J., and Robinson, C. (2005). Climate change and marine plankton. *Trends Ecol. Evol.* *20*, 337–344.
- Hutchins, D.A., and Fu, F. (2017). Microorganisms and ocean global change. *Nat. Microbiol.* *26*, 1–11.
- Keeling, P.J., Burki, F., Wilcox, H.M., Allam, B., Allen, E.E., Amaral-Zettler, L.A., Armbrust, E.V., Archibald, J.M., Bharti, A.K., Bell, C.J., et al. (2014). The marine microbial eukaryote transcriptome sequencing project (MMETSP): illuminating the functional diversity of eukaryotic life in the oceans through transcriptome sequencing. *PLoS Biol.* *12*, e1001889.
- Johnson, L.K., Alexander, H., and Brown, C.T. (2019). Re-assembly, quality evaluation, and annotation of 678 microbial eukaryotic reference transcriptomes. *Gigascience* *8*, 1–12.
- Palenik, B., Grimwood, J., Aerts, A., Rouzé, P., Salamov, A., Putnam, N., Dupont, C., Jorgensen, R., Derelle, E., Rombauts, S., et al. (2007). The tiny eukaryote *Ostreococcus* provides genomic insights into the paradox of plankton speciation. *Proc. Natl. Acad. Sci. U S A* *104*, 7705–7710.
- Bowler, C., Allen, A.E., Badger, J.H., Grimwood, J., Jabbari, K., Kuo, A., Maheswari, U., Martens, C., Maumus, F., Otilar, R.P., et al. (2008). The *Phaeodactylum* genome reveals the evolutionary history of diatom genomes. *Nature* *456*, 239–244.
- Worden, A.Z., Lee, J.H., Mock, T., Rouzé, P., Simmons, M.P., Aerts, A.L., Allen, A.E., Cuvelier, M.L., Derelle, E., Everett, M.V., et al. (2009). Green evolution and dynamic adaptations revealed by genomes of the marine picoeukaryotes *Micromonas*. *Science* *324*, 268–272.
- Sunagawa, S., Coelho, L.P., Chaffron, S., Kultima, J.R., Labadie, K., Salazar, G., Djahanschiri, B., Zeller, G., Mende, D.R., Alberti, A., et al. (2015). Ocean plankton. Structure and function of the global ocean microbiome. *Science* *348*, 1261359.
- Sieracki, M.E., Poulton, N.J., Jaillon, O., Wincker, P., de Vargas, C., Rubinat-Ripoll, L., Stepanauskas, R., Logares, R., and Massana, R. (2019). Single cell genomics yields a wide diversity of small planktonic protists across major ocean ecosystems. *Sci. Rep.* *9*, 1–11.
- Sibbald, S.J., and Archibald, J.M. (2017). More protist genomes needed. *Nat. Ecol. Evol.* *1*, 145.
- Del Campo, J., Sieracki, M.E., Molestina, R., Keeling, P., Massana, R., and Ruiz-Trillo, I. (2014). The others: our biased perspective of eukaryotic genomes. *Trends Ecol. Evol.* *29*, 252.
- Sunagawa, S., Acinas, S.G., Bork, P., Bowler, C., Eveillard, D., Gorsky, G., Guidi, L., Iudicone, D., Karsenti, E., Lombard, F., et al. (2020). *Tara Oceans*: towards global ocean ecosystems biology. *Nat. Rev. Microbiol.* *18*, 428–445.
- Vorobev, A., Dupouy, M., Carradec, Q., Delmont, T.O., Annamali, A., Wincker, P., and Pelletier, E. (2020). Transcriptome reconstruction and functional analysis of eukaryotic marine plankton communities via high-throughput metagenomics and metatranscriptomics. *Genome Res.* *30*, 647–659.
- Richter, D., Watteaux, R., Vannier, T., Leconte, J., Frémont, P., Reygondeau, G., Maillat, N., Henry, N., Benoit, G., Fernández-Guerra, A., et al. (2019). Genomic evidence for global ocean plankton biogeography shaped by large-scale current systems. Preprint at bioRxiv. <https://doi.org/10.1101/867739> 23, 31.
- Frémont, P., Gehlen, M., Vrac, M., Leconte, J., Delmont, T.O., Wincker, P., et al. (2022). Restructuring of plankton genomic biogeography in the

- surface ocean under climate change. *Nature Climate Change* 12 (4), 393–401. <https://doi.org/10.1038/s41558-022-01314-8>.
25. Tyson, G.W., Chapman, J., Hugenholtz, P., Allen, E.E., Ram, R.J., Richardson, P.M., Solovyev, V.V., Rubin, E.M., Rokhsar, D.S., and Banfield, J.F. (2004). Community structure and metabolism through reconstruction of microbial genomes from the environment. *Nature* 428, 37–43.
 26. Delmont, T.O., Quince, C., Shaiber, A., Esen, Ö.C., Lee, S.T., Rappé, M.S., MacLellan, S.L., Lückner, S., and Eren, A.M. (2018). Nitrogen-fixing populations of Planctomycetes and Proteobacteria are abundant in surface ocean metagenomes. *Nat. Microbiol.* 37, 804–813.
 27. Tully, B.J., Graham, E.D., and Heidelberg, J.F. (2018). The reconstruction of 2,631 draft metagenome-assembled genomes from the global oceans. *Sci. Data* 51, 1–8.
 28. Tully, B.J. (2019). Metabolic diversity within the globally abundant Marine Group II Euryarchaea offers insight into ecological patterns. *Nat. Commun.* 107, 1–12.
 29. Gregory, A.C., Zayed, A.A., Conceição-Neto, N., Temperton, B., Bolduc, B., Alberti, A., Ardyna, M., Arkhipova, K., Carmichael, M., Cruaud, C., et al. (2019). Marine DNA viral macro- and microdiversity from Pole to Pole. *Cell* 177, 1109–1123.e14.
 30. Moniruzzaman, M., Martinez-Gutierrez, C.A., Weinheimer, A.R., and Aylward, F.O. (2020). Dynamic genome evolution and complex virocell metabolism of globally-distributed giant viruses. *Nat. Commun.* 111, 1–11.
 31. Parks, D.H., Rinke, C., Chuvochina, M., Chaumeil, P.A., Woodcroft, B.J., Evans, P.N., Hugenholtz, P., and Tyson, G.W. (2017). Recovery of nearly 8,000 metagenome-assembled genomes substantially expands the tree of life. *Nat. Microbiol.* 2, 1533–1542.
 32. Delmont, T.O., Murat Eren, A., Vineis, J.H., and Post, A.F. (2015). Genome reconstructions indicate the partitioning of ecological functions inside a phytoplankton bloom in the Amundsen Sea, Antarctica. *Front. Microbiol.* 6, 1090.
 33. Olm, M.R., West, P.T., Brooks, B., Firek, B.A., Baker, R., Morowitz, M.J., and Banfield, J.F. (2019). Genome-resolved metagenomics of eukaryotic populations during early colonization of premature infants and in hospital rooms. *Microbiome* 7, 1–16.
 34. West, P.T., Probst, A.J., Grigoriev, I.V., Thomas, B.C., and Banfield, J.F. (2018). Genome-reconstruction for eukaryotes from complex natural microbial communities. *Genome Res.* 28, gr.228429.117.
 35. Duncan, A., Barry, K., Daum, C., Eloë-Fadrosh, E., Roux, S., Tringe, S.G., Schmidt, K., Valentin, K.U., Varghese, N., Grigoriev, I.V., et al. (2020). Metagenome-assembled genomes of phytoplankton communities across the Arctic Circle. Preprint at bioRxiv. <https://doi.org/10.1101/2020.06.16.154583>.
 36. Biscotti, M.A., Olmo, E., and Heslop-Harrison, J.S. (2015). Repetitive DNA in eukaryotic genomes. *Chromosome Res.* 23, 415–420.
 37. Gregory, T.R. (2005). Synergy between sequence and size in Large-scale genomics. *Nat. Rev. Genet.* 6, 699–708.
 38. Eren, A.M., Esen, Ö.C., Quince, C., Vineis, J.H., Morrison, H.G., Sogin, M.L., and Delmont, T.O. (2015). Anvi'o: an advanced analysis and visualization platform for 'omics data. *PeerJ* 3, e1319.
 39. Eren, A.M., Kiefl, E., Shaiber, A., Veseli, I., Miller, S.E., Schechter, M.S., Fink, I., Pan, J.N., Yousef, M., Fogarty, E.C., et al. (2020). Community-led, integrated, reproducible multi-omics with anvi'o. *Nat. Microbiol.* 6, 3–6.
 40. Niang, G., Hoebeke, M., Meng, A., Liu, X., Scheremetjew, M., Finn, R., Pelletier, E., and Erwan, C. METdb, an extended reference resource for Marine Eukaryote Transcriptomes, (unpublished). <http://metdb.sb-roscoff.fr/metdb/>.
 41. Delmont, T.O., Pierella Karlusich, J.J., Veseli, I., Fuessel, J., Eren, A.M., Foster, R.A., Bowler, C., Wincker, P., and Pelletier, E. (2021). Heterotrophic bacterial diazotrophs are more abundant than their cyanobacterial counterparts in metagenomes covering most of the sunlit ocean. *ISME J.* 2021, 1–10.
 42. Delmont, T.O. (2021). Discovery of nondiazotrophic *Trichodesmium* species abundant and widespread in the open ocean. *Proc. Natl. Acad. Sci. U S A* 118, e2112355118.
 43. Gaia, M., Meng, L., Pelletier, E., Forterre, P., Vanni, C., Fernandez-Guerra, A., Jaillon, O., Wincker, P., Ogata, H., and Delmont, T.O. (2021). Discovery of a class of giant virus relatives displaying unusual functional traits and prevalent within plankton: the mirusviricetes. Preprint at bioRxiv. <https://doi.org/10.1101/2021.12.27.474232>.
 44. Martinez-Gutierrez, C.A., and Aylward, F.O. (2021). Phylogenetic signal, congruence, and uncertainty across bacteria and archaea. *Mol. Biol. Evol.* 38, 5514–5527.
 45. Guglielmini, J., Woo, A.C., Krupovic, M., Forterre, P., and Gaia, M. (2019). Diversification of giant and large eukaryotic dsDNA viruses predated the origin of modern eukaryotes. *Proc. Natl. Acad. Sci. U S A* 116, 19585–19592.
 46. Burki, F., Roger, A.J., Brown, M.W., and Simpson, A.G.B. (2020). The new tree of eukaryotes. *Trends Ecol. Evol.* 35, 43–55.
 47. Humes, A.G. (1994). How many copepods?. *Ecology and Morphology of Copepods*, pp. 1–7.
 48. Kjørboe, T. (2011). What makes pelagic copepods so successful? *J. Plankton Res.* 33, 677–685.
 49. Steinberg, D.K., and Landry, M.R. (2017). Zooplankton and the ocean carbon cycle. *Ann. Rev. Mar. Sci.* 9, 413–444.
 50. Jørgensen, T.S., Nielsen, B.L.H., Petersen, B., Browne, P.D., Hansen, B.W., and Hansen, L.H. (2019). The whole genome sequence and mRNA transcriptome of the tropical cyclopoid copepod *apocyclops royi*. *G3 (Bethesda)* 9, 1295–1302.
 51. Jørgensen, T.S., Petersen, B., Petersen, H.C.B., Browne, P.D., Prost, S., Stillman, J.H., Hansen, L.H., and Hansen, B.W. (2019). The genome and mRNA transcriptome of the cosmopolitan calanoid copepod *Acartia tonsa* dana improve the understanding of copepod genome size evolution. *Genome Biol. Evol.* 11, 1440–1450.
 52. Malviya, S., Scalco, E., Audic, S., Vincent, F., Veluchamy, A., Poulain, J., Wincker, P., Iudicone, D., De Vargas, C., Bittner, L., et al. (2016). Insights into global diatom distribution and diversity in the world's ocean. *Proc. Natl. Acad. Sci. U S A* 113, E1516–E1525.
 53. Costa, R.R., Mendes, C.R.B., Tavano, V.M., Dotto, T.S., Kerr, R., Monteiro, T., Odebrecht, C., and Secchi, E.R. (2020). Dynamics of an intense diatom bloom in the northern antarctic peninsula, february 2016. *Limnol. Oceanogr.* 65, 2056–2075.
 54. Schön, M.E., Zlatogursky, V.V., Singh, R.P., Poirier, C., Wilken, S., Mathur, V., Strassert, J.F.H., Pinhassi, J., Worden, A.Z., Keeling, P.J., et al. (2021). Single cell genomics reveals plastid-lacking Picozoa are close relatives of red algae. *Nat. Commun.* 12, 1–10.
 55. Massana, R., Del Campo, J., Sieracki, M.E., Audic, S., and Logares, R. (2014). Exploring the uncultured microeukaryote majority in the oceans: reevaluation of ribogroups within stramenopiles. *ISME J.* 8, 854.
 56. Song, B., Chen, S., and Chen, W. (2018). Dinoflagellates, a unique lineage for retrogene Research. *Front. Microbiol.* 9, 1556.
 57. Huerta-Cepas, J., Szklarczyk, D., Heller, D., Hernández-Plaza, A., Forslund, S.K., Cook, H., Mende, D.R., Letunic, I., Rattei, T., Jensen, L.J., et al. (2019). eggNOG 5.0: a hierarchical, functionally and phylogenetically annotated orthology resource based on 5090 organisms and 2502 viruses. *Nucleic Acids Res.* 47, D309–D314.
 58. Huerta-Cepas, J., Forslund, K., Coelho, L.P., Szklarczyk, D., Jensen, L.J., Von Mering, C., and Bork, P. (2017). Fast genome-wide functional annotation through orthology assignment by eggNOG-mapper. *Mol. Biol. Evol.* 34, 2115–2122.
 59. Jensen, L.J., Julien, P., Kuhn, M., von Mering, C., Muller, J., Doerks, T., and Bork, P. (2008). eggNOG: automated construction and annotation of orthologous groups of genes. *Nucleic Acids Res.* 36, D250–D254.

60. Delmont, T.O., and Eren, E.M. (2018). Linking pangenomes and metagenomes: the *Prochlorococcus* metapangenome. *PeerJ* 6, e4320.
61. Seeleuthner, Y., Mondy, S., Lombard, V., Carradec, Q., Pelletier, E., Wessner, M., Leconte, J., Mangot, J.F., Poulain, J., Labadie, K., et al. (2018). Single-cell genomics of multiple uncultured stramenopiles reveals underestimated functional diversity across oceans. *Nat. Commun.* 9, 1–10.
62. Hill, K., Hemmler, R., Kovermann, P., Calenberg, M., Kreimer, G., and Wagner, R. (2000). A Ca(2+)- and voltage-modulated flagellar ion channel is a component of the mechanoshock response in the unicellular green alga *Spermatozopsis similis*. *Biochim. Biophys. Acta* 1466, 187–204.
63. Wood, V., Lock, A., Harris, M.A., Rutherford, K., Bähler, J., and Oliver, S.G. (2019). Hidden in plain sight: what remains to be discovered in the eukaryotic proteome? *Open Biol.* 9, 180241.
64. Vanni, C., Schechter, M.S., Acinas, S.G., Barberán, A., Buttigieg, P.L., Casamayor, E.O., et al. (2022). Unifying the known and unknown microbial coding sequence space. *eLife* 11. <https://doi.org/10.7554/ELIFE.67667>.
65. Ibarbalz, F.M., Henry, N., Brandão, M.C., Martini, S., Busseni, G., Byrne, H., Coelho, L.P., Endo, H., Gasol, J.M., Gregory, A.C., et al. (2019). Global trends in marine plankton diversity across kingdoms of life. *Cell* 179, 1084–1097.e21.
66. Guérin, N., Ciccarella, M., Flamant, E., Frémont, P., Mangenot, S., Istace, B., Noel, B., Romac, S., Bachy, C., Gachenot, M., et al. (2021). Genomic adaptation of the picoeukaryote *Pelagomonas calceolata* to iron-poor oceans revealed by a chromosome-scale genome sequence. Preprint at bioRxiv. <https://doi.org/10.1101/2021.10.25.465678>.
67. Saary, P., Mitchell, A.L., and Finn, R.D. (2020). Estimating the quality of eukaryotic genomes recovered from metagenomic analysis with EukCC. *Genome Biol.* 21, 1–21.
68. Alexander, H., Hu, S.K., Krinos, A.I., Pachiadaki, M., Tully, B.J., Neely, C.J., and Reiter, T. (2021). Eukaryotic genomes from a global metagenomic dataset illuminate trophic modes and biogeography of ocean plankton. Preprint at bioRxiv. <https://doi.org/10.1101/2021.07.25.453713>.
69. Archibald, J.M., and Keeling, P.J. (2002). Recycled plastids: a “green movement” in eukaryotic evolution. *Trends Genet.* 18, 577–584.
70. Deschamps, P., and Moreira, D. (2012). Reevaluating the green contribution to diatom genomes. *Genome Biol. Evol.* 4, 683–688.
71. Keeling, P.J. (2013). The number, speed, and impact of plastid endosymbioses in eukaryotic evolution. *Annu. Rev. Plant Biol.* 64, 583–607.
72. Reyes-Prieto, A., Weber, A.P.M., and Bhattacharya, D. (2007). The origin and establishment of the plastid in algae and plants. *Annu. Rev. Genet.* 41, 147–168.
73. Derelle, R., López-García, P., Timpano, H., and Moreira, D. (2016). A phylogenomic framework to study the diversity and evolution of stramenopiles (=Heterokonts). *Mol. Biol. Evol.* 33, 2890–2898.
74. Emery, N.J., and Clayton, N.S. (2004). The mentality of crows: convergent evolution of intelligence in corvids and apes. *Science* 306, 1903–1907.
75. Zakon, H.H. (2002). Convergent evolution on the molecular level. *Brain Behav. Evol.* 59, 250–261.
76. Leander, B.S. (2008). A hierarchical view of convergent evolution in microbial eukaryotes. *J. Eukaryot. Microbiol.* 55, 59–68.
77. Keeling, P.J., and Palmer, J.D. (2008). Horizontal gene transfer in eukaryotic evolution. *Nat. Rev. Genet.* 9, 605–618.
78. Danchin, E.G.J. (2016). Lateral gene transfer in eukaryotes: tip of the iceberg or of the ice cube. *BMC Biol.* 14, 1–3.
79. Andersson, J.O. (2006). Convergent evolution: gene sharing by eukaryotic plant pathogens. *Curr. Biol.* 16, R804–R806.
80. Dunning, L.T., Olofsson, J.K., Parisod, C., Choudhury, R.R., Moreno-Villena, J.J., Yang, Y., Dionora, J., Paul Quick, W., Park, M., Bennetzen, J.L., et al. (2019). Lateral transfers of large DNA fragments spread functional genes among grasses. *Proc. Natl. Acad. Sci. U S A* 116, 4416–4425.
81. Chan, C.X., Bhattacharya, D., and Reyes-Prieto, A. (2012). Endosymbiotic and horizontal gene transfer in microbial eukaryotes: impacts on cell evolution and the tree of life. *Mob. Genet. Elem.* 2, 101.
82. Dorrell, R.G., Gile, G., McCallum, G., Méheust, R., Bapteste, E.P., Klinger, C.M., Brillet-Guéguen, L., Freeman, K.D., Richter, D.J., and Bowler, C. (2017). Chimeric origins of ochrophytes and haptophytes revealed through an ancient plastid proteome. *eLife* 6, e23717.
83. Martin, W.F. (2017). Too much eukaryote LGT. *BioEssays* 39, 1700115.
84. Leger, M.M., Eme, L., Stairs, C.W., and Roger, A.J. (2018). Demystifying eukaryote lateral gene transfer (response to martin 2017). *BioEssays* 40, 1700242. <https://doi.org/10.1002/bies.201700115>.
85. Zmasek, C.M., and Godzik, A. (2011). Strong functional patterns in the evolution of eukaryotic genomes revealed by the reconstruction of ancestral protein domain repertoires. *Genome Biol.* 12, 1–13.
86. Li, D., Liu, C.M., Luo, R., Sadakane, K., and Lam, T.W. (2014). MEGAHIT: an ultra-fast single-node solution for large and complex metagenomics assembly via succinct de Bruijn graph. *Bioinformatics* 31, 1674–1676.
87. Hyatt, D., Chen, G.-L., Locascio, P.F., Land, M.L., Larimer, F.W., and Hauser, L.J. (2010). Prodigal: prokaryotic gene recognition and translation initiation site identification. *BMC Bioinf.* 11, 119.
88. Eddy, S.R. (2011). Accelerated profile HMM searches. *PLoS Comput. Biol.* 7, e1002195.
89. Simão, F.A., Waterhouse, R.M., Ioannidis, P., Kriventseva, E.V., and Zdobnov, E.M. (2015). BUSCO: assessing genome assembly and annotation completeness with single-copy orthologs. *Bioinformatics* 31, 3210–3212.
90. Delmont, T.O. (2018). Assessing the completion of eukaryotic bins with anvio. *Blog post*. <http://merenlab.org/2018/05/05/eukaryotic-single-copy-core-genes/>.
91. Li, H., and Durbin, R. (2009). Fast and accurate short read alignment with Burrows-Wheeler transform. *Bioinformatics* 25, 1754–1760.
92. Li, H., Handsaker, B., Wysoker, A., Fennell, T., Ruan, J., Homer, N., Marth, G., Abecasis, G., and Durbin, R. (2009). The sequence alignment/map format and SAMtools. *Bioinformatics* 25, 2078–2079.
93. Alneberg, J., Bjarnason, B.S., de Bruijn, I., Schirmer, M., Quick, J., Ijaz, U.Z., Lahti, L., Loman, N.J., Andersson, A.F., and Quince, C. (2014). Binning metagenomic contigs by coverage and composition. *Nat. Methods* 11, 1144–1146.
94. Delmont, T.O., and Eren, A.M. (2016). Identifying contamination with advanced visualization and analysis practices: metagenomic approaches for eukaryotic genome assemblies. *PeerJ* 4, e1839.
95. Mangot, J.F., Logares, R., Sánchez, P., Latorre, F., Seeleuthner, Y., Mondy, S., Sieracki, M.E., Jaillon, O., Wincker, P., Vargas, C., et al. (2017). Accessing the genomic information of unculturable oceanic picoeukaryotes by combining multiple single cells. *Sci. Rep.* 7, 41498.
96. López-Escardó, D., Grau-Bové, X., Guillaumet-Adkins, A., Gut, M., Sieracki, M.E., and Ruiz-Trillo, I. (2017). Evaluation of single-cell genomics to address evolutionary questions using three SAGs of the choanoflagellate *Monosiga brevicollis*. *Sci. Rep.* 7, 11025.
97. Vannier, T., Leconte, J., Seeleuthner, Y., Mondy, S., Pelletier, E., Aury, J.M., De Vargas, C., Sieracki, M., Ludicone, D., Vaalot, D., et al. (2016). Survey of the green picoalga *Bathycoccus* genomes in the global ocean. *Sci. Rep.* 6, 37900.
98. Delcher, A.L., Phillippy, A., Carlton, J., and Salzberg, S.L. (2002). Fast algorithms for large-scale genome alignment and comparison. *Nucleic Acids Res.* 30, 2478–2483.
99. Levy Karin, E., Mirdita, M., and Söding, J. (2020). MetaEuk-sensitive, high-throughput gene discovery, and annotation for large-scale eukaryotic metagenomics. *Microbiome* 8, 1–15.

100. Birney, E., Clamp, M., and Durbin, R. (2004). GeneWise and genomewise. *Genome Res.* *14*, 988–995.
101. Li, H. (2018). Minimap2: pairwise alignment for nucleotide sequences. *Bioinformatics* *34*, 3094–3100.
102. Stanke, M., Keller, O., Gunduz, I., Hayes, A., Waack, S., and Morgenstern, B. (2006). AUGUSTUS: ab initio prediction of alternative transcripts. *Nucleic Acids Res.* *34*, W435–W439.
103. Kent, W.J. (2002). BLAT—the BLAST-like alignment tool. *Genome Res.* *12*, 656–664.
104. Dobin, A., Davis, C.A., Schlesinger, F., Drenkow, J., Zaleski, C., Jha, S., Batut, P., Chaisson, M., and Gingeras, T.R. (2013). STAR: ultrafast universal RNA-seq aligner. *Bioinformatics* *29*, 15–21.
105. Denoeud, F., Aury, J.M., Da Silva, C., Noel, B., Rogier, O., Delledonne, M., Morgante, M., Valle, G., Wincker, P., Scarpelli, C., et al. (2008). Annotating genomes with massive-scale RNA sequencing. *Genome Biol.* *9*, 1–12.
106. Korf, I. (2004). Gene finding in novel genomes. *BMC Bioinf.* *5*, 1–9.
107. Boyer, T.P., Antonov, J.I., Baranova, O.K., Coleman, C., Garcia, H.E., Grodsky, A., et al. (2013). In *WORLD OCEAN DATABASE 2013*, NOAA Atlas NESDIS 72, S. Levitus, ed. (Alexey Mishonoc, Tech. Ed), pp. 1–208.
108. Aumont, O., Ethé, C., Tagliabue, A., Bopp, L., and Gehlen, M. (2015). PISCES-v2: an ocean biogeochemical model for carbon and ecosystem studies. *Geosci. Model. Dev.* *8*, 2465–2513.
109. Da Cunha, V., Gaia, M., Nasir, A., and Forterre, P. (2018). Asgard archaea do not close the debate about the universal tree of life topology. *PLoS Genet.* *14*, e1007215.
110. Camacho, C., Coulouris, G., Avagyan, V., Ma, N., Papadopoulos, J., Bealer, K., and Madden, T.L. (2009). BLAST+: architecture and applications. *BMC Bioinf.* *10*, 1–9.
111. Katoh, K., and Standley, D.M. (2013). MAFFT multiple sequence alignment software version 7: improvements in performance and usability. *Mol. Biol. Evol.* *30*, 772–780.
112. Nguyen, L.T., Schmidt, H.A., Von Haeseler, A., and Minh, B.Q. (2015). IQ-TREE: a fast and effective stochastic algorithm for estimating maximum-likelihood phylogenies. *Mol. Biol. Evol.* *32*, 268–274.
113. Kalyaanamoorthy, S., Minh, B.Q., Wong, T.K.F., Von Haeseler, A., and Jermiin, L.S. (2017). ModelFinder: fast model selection for accurate phylogenetic estimates. *Nat. Methods* *14*, 587–589.
114. Guindon, S., Dufayard, J.F., Lefort, V., Anisimova, M., Hordijk, W., and Gascuel, O. (2010). New algorithms and methods to estimate maximum-likelihood phylogenies: assessing the performance of PhyML 3.0. *Syst. Biol.* *59*, 307–321.
115. Hoang, D.T., Chernomor, O., Von Haeseler, A., Minh, B.Q., and Vinh, L.S. (2018). UFBoot2: improving the ultrafast bootstrap approximation. *Mol. Biol. Evol.* *35*, 518–522.
116. Buchfink, B., Xie, C., and Huson, D.H. (2015). Fast and sensitive protein alignment using DIAMOND. *Nat. Methods* *12*, 59–60.

STAR★METHODS

KEY RESOURCES TABLE

REAGENT or RESOURCE	SOURCE	IDENTIFIER
Deposited data		
Data generated in this study	This paper	https://www.genoscope.cns.fr/tara/
Data needed for the Agnostos related analyses for this study	This paper	https://figshare.com/articles/dataset/Delmont_et_al_2022/19403531
Software and algorithms		
Anvi'o	Eren et al. 2021	https://anvio.org/
Agnostos	Vanni et al., 2021	https://github.com/functional-dark-side/agnostos-wf
Custom codes required to perform analyses related to Agnostos in this study	This paper	https://zenodo.org/record/6379623

RESOURCE AVAILABILITY

Lead contact

Further information and requests for resources and analyses should be directed to and will be fulfilled by the lead contact, Tom O. Delmont (Tom.Delmont@genoscope.fr).

Materials availability

This study did not generate new materials.

Data and code availability

- All data our study generated are publicly available at <http://www.genoscope.cns.fr/tara/>. The link provides access to the 11 raw metagenomic co-assemblies, the FASTA files for 713 MAGs and SAGs, the ~10 million protein-coding sequences (nucleotides, amino acids and gff format), and the curated DNA-dependent RNA polymerase genes (MAGs and SAGs and METdb transcripts). This link also provides access to the supplemental figures and the [Supplemental material](#). Finally, code development within anvi'o for the BUSCO single copy core genes is available at <https://github.com/merenlab/anvio>.
- Original code has been deposited at Zenodo and is publicly available. The accession number is listed in the [key resources table](#).
- Any additional information required to reanalyze the data reported in this paper is available from the [lead contact](#) upon request.

METHOD DETAILS

Tara Oceans metagenomes

We analyzed a total of 939 *Tara Oceans* metagenomes available at the EBI under project PRJEB402 (<https://www.ebi.ac.uk/ena/browser/view/PRJEB402>). 265 of these metagenomes have been released through this study. [Table S1](#) reports accession numbers and additional information (including the number of reads and environmental metadata) for each metagenome.

Genome-resolved metagenomics

We organized the 798 metagenomes corresponding to size fractions ranging from 0.8 μm to 2 mm into 11 'metagenomic sets' based upon their geographic coordinates. We used those 0.28 trillion reads as inputs for 11 metagenomic co-assemblies using MEGAHIT⁸⁶ v1.1.1, and simplified the scaffold header names in the resulting assembly outputs using anvi'o^{38,39} v.6.1 (available from <http://merenlab.org/software/anvio>). Co-assemblies yielded 78 million scaffolds longer than 1,000 nucleotides for a total volume of 150.7 Gbp. We performed a combination of automatic and manual binning on each co-assembly output, focusing only on the 11.9 million scaffolds longer than 2,500 nucleotides, which resulted in 837 manually curated eukaryotic metagenome-assembled genomes (MAGs) longer than 10 million nucleotides. Briefly, (1) anvi'o profiled the scaffolds using Prodigal⁸⁷ v2.6.3 with default parameters to identify an initial set of genes, and HMMER⁸⁸ v3.1b2 to detect genes matching to 83 single-copy core gene markers from BUSCO⁸⁹ (benchmarking is described in a dedicated blog post⁹⁰), (2) we used a customized database including both NCBI's NT database and METdb to infer the taxonomy of genes with a Last Common Ancestor strategy⁵ (results were imported as described in <http://merenlab.org/2016/06/18/importing-taxonomy>), (3) we mapped short reads from the metagenomic set to the scaffolds using BWA v0.7.15⁹¹ (minimum identity of 95%) and stored the recruited reads as BAM files using samtools,⁹² (4) anvi'o profiled each BAM file to estimate the coverage and detection statistics of each scaffold, and combined mapping profiles into a merged profile database

for each metagenomic set. We then clustered scaffolds with the automatic binning algorithm CONCOCT⁹³ by constraining the number of clusters (thereafter dubbed metabins) per metagenomic set to a number ranging from 50 to 400 depending on the set. Each metabin ($n = 2,550$, ~ 12 million scaffolds) was manually binned using the *anvi'o* interactive interface. The interface considers the sequence composition, differential coverage, GC-content, and taxonomic signal of each scaffold. Finally, we individually refined each eukaryotic MAG >10 Mbp as outlined in Delmont and Eren,⁹⁴ and renamed scaffolds they contained according to their MAG ID. [Table S2](#) reports the genomic features (including completion and redundancy values) of the eukaryotic MAGs. For details on our protocol used for binning and curation of metabins, see [Methods S1](#), [Supplemental methods](#), Related to the [STAR Methods](#).

A first gigabase scale eukaryotic MAG

We performed targeted genome-resolved metagenomics to confirm the biological relevance and improve statistics of the single MAG longer than one Gbp with an additional co-assembly (five Southern Ocean metagenomes for which this MAG had average vertical coverage >1x) and by considering contigs longer than 1,000 nucleotides, leading to a gain of 181,8 million nucleotides. To our knowledge, we describe here the first successful characterization of a Gigabase-scale MAG (1.32 Gbp with 419,520 scaffolds), which we could identify using two distinct metagenomic co-assemblies.

MAGs from the 0.2–3 μm size fraction

We incorporated into our database 20 eukaryotic MAGs longer than 10 million nucleotides previously characterized from the 0.2–3 μm size fraction,²⁶ providing a set of MAGs corresponding to eukaryotic cells ranging from 0.2 μm (picoeukaryotes) to 2 mm (small animals).

Single-cell genomics

We used 158 eukaryotic single cells sorted by flow cytometry from seven *Tara* Oceans stations as input to perform genomic assemblies (up to 18 cells with identical 18S rRNA genes per assembly to optimize completion statistics, see [Table S2](#)), providing 34 single-cell genomes (SAGs) longer than 10 million nucleotides. Cell sorting, DNA amplification, sequencing and assembly were performed as described elsewhere.¹⁸ In addition, manual curation was performed using sequence composition and differential coverage across 100 metagenomes in which the SAGs were most detected, following the methodology described in the [genome-resolved metagenomics](#) section. For SAGs with no detection in *Tara* Oceans metagenomes, only sequence composition and taxonomical signal could be used, limiting this curation effort's scope. Notably, manual curation of SAGs using the genome-resolved metagenomic workflow turned out to be highly valuable, leading to the removal of more than one hundred thousand scaffolds for a total volume of 193.1 million nucleotides. This metagenomic-guided decontamination effort contributes to previous efforts characterizing eukaryotic SAGs from the same cell sorting material^{18,61,95–97} and provides new marine eukaryotic guidelines for SAGs. For details on our protocol used for curation of eukaryotic SAGs, see [Methods S1](#), [Supplemental methods](#), Related to the [STAR Methods](#).

Characterization of a non-redundant database of MAGs and SAGs

We determined the average nucleotide identity (ANI) of each pair of MAGs and SAGs using the *dnadiff* tool from the MUMmer package⁹⁸ v.4.0b2. MAGs and SAGs were considered redundant when their ANI was >98% (minimum alignment of >25% of the smaller MAG or SAG in each comparison). We then selected the longest MAG or SAG to represent a group of redundant MAGs and SAGs. This analysis provided a non-redundant genomic database of 713 MAGs and SAGs.

Taxonomical inference of MAGs and SAGs

We manually determined the taxonomy of MAGs and SAGs using a combination of approaches: (1) taxonomical signal from the initial gene calling (*Prodigal*), (2) phylogenetic approaches using the RNA polymerase genes and METdb, (3) ANI within the MAGs and SAGs and between MAGs and SAGs and METdb, (4) local blasts using BUSCO gene markers, (5) and lastly the functional clustering of MAGs and SAGs to gain knowledge into very few MAGs and SAGs lacking gene markers and ANI signal. In addition, Picozoa SAGs⁵⁴ were used to identify MAGs from this phylum lacking representatives in METdb. For details on METdb, see [Methods S1](#), [Supplemental methods](#), Related to the [STAR Methods](#).

Protein coding genes

Protein coding genes for the MAGs and SAGs were characterized using three complementary approaches: protein alignments using reference databases, metatranscriptomic mapping from *Tara* Oceans and *ab-initio* gene predictions. While the overall framework was highly similar for MAGs and SAGs, the methodology slightly differed to take the best advantage of those two databases when they were processed (see the two following sections).

Protein-coding genes for the MAGs

Protein alignments

Since the alignment of a large protein database on all the MAG assemblies is time greedy, we first detected the potential proteins of Uniref. 90 + METdb that could be aligned to the assembly by using *MetaEuk*⁹⁹ with default parameters. This subset of proteins was aligned using BLAT with default parameters, which localized each protein on the MAG assembly. The exon/intron structure was

refined using geneWise¹⁰⁰ with default parameters to detect splice sites accurately. Each MAG's GeneWise alignments were converted into a standard GFF file and given as input to gmove.

Metatranscriptomic mapping from Tara Oceans

A total of 905 individual *Tara* Oceans metatranscriptomic assemblies (mostly from large planktonic size fractions) were aligned on each MAG assembly using Minimap2¹⁰¹ (version 2.15-r905) with the “-ax splice” flag. BAM files were filtered as follows: low complexity alignments were removed and only alignments covering at least 80% of a given metatranscriptomic contig with at least 95% of identity were retained. The BAM files were converted into a standard GFF file and given as input to gmove.

Ab-initio gene predictions

A first gene prediction for each MAG was performed using gmove and the GFF file generated from metatranscriptomic alignments. From these preliminary gene models, 300 gene models with a start and a stop codon were randomly selected and used to train AUGUSTUS¹⁰² (version 3.3.3). A second time, AUGUSTUS was launched on each MAG assembly using the dedicated calibration file, and output files were converted into standard GFF files and given as input to gmove. Each individual line of evidence was used as input for gmove (<http://www.genoscope.cns.fr/externe/gmove/>) with default parameters to generate the final protein-coding genes annotations.

Protein coding genes for the SAGs

Protein alignments

The Uniref90 + METdb database of proteins was aligned using BLAT¹⁰³ with default parameters, which localized protein on each SAG assembly. The exon/intron structure was refined using GeneWise¹⁰⁰ and default parameters to detect splice sites accurately. The GeneWise alignments of each SAG were converted into a standard GFF file and given as input to gmove.

Metatranscriptomic mapping from Tara Oceans

The 905 *Tara* Oceans metatranscriptomic individual fastq files were filtered with kfir (<http://www.genoscope.cns.fr/kfir>) using a k-mer approach to select only reads that shared 25-mer with the input SAG assembly. This subset of reads was aligned on the corresponding SAG assembly using STAR¹⁰⁴ (version 2.5.2.b) with default parameters. BAM files were filtered as follows: low complexity alignments were removed and only alignments covering at least 80% of the metatranscriptomic reads with at least 90% of identity were retained. Candidate introns and exons were extracted from the BAM files and given as input to gmove.¹⁰⁵

Ab-initio gene predictions

Ab-initio models were predicted using SNAP¹⁰⁶ (v2013-02-16) trained on complete protein matches and gmove models, and output files were converted into standard GFF files and given as input to gmove. Each line of evidence was used as input for gmove (<http://www.genoscope.cns.fr/externe/gmove/>) with default parameters to generate the final protein-coding genes annotations.

BUSCO completion scores for protein-coding genes in MAGs and SAGs

BUSCO⁸⁹ v.3.0.4 was used with the set of eukaryotic single-copy core gene markers (n = 255). Completion and redundancy (number of duplicated gene markers) of MAGs and SAGs were computed from this analysis.

Biogeography of MAGs and SAGs

We performed a final mapping of all metagenomes to calculate the mean coverage and detection of the MAGs and SAGs (Table S5). Briefly, we used BWA v0.7.15 (minimum identity of 90%) and a FASTA file containing the 713 non-redundant MAGs and SAGs to recruit short reads from all 939 metagenomes. We considered MAGs and SAGs were detected in a given filter when >25% of their length was covered by reads to minimize non-specific read recruitments.²⁶ The number of recruited reads below this cut-off was set to 0 before determining vertical coverage and percent of recruited reads. Regarding the projection of mapped reads, if MAGs and SAGs were to be complete, we used BUSCO completion scores to project the number of mapped reads. Note that we preserved the actual number of mapped reads for the MAGs and SAGs with completion <10% to avoid substantial errors to be made in the projections.

Identifying the environmental niche of MAGs and SAGs

Seven physicochemical parameters were used to define environmental niches: sea surface temperature (SST), salinity (Sal), dissolved silica (Si), nitrate (NO₃), phosphate (PO₄), iron (Fe), and a seasonality index of nitrate (SI NO₃). Except for Fe and SI NO₃, these parameters were extracted from the gridded World Ocean Atlas 2013 (WOA13).¹⁰⁷ Climatological Fe fields were provided by the biogeochemical model PISCES-v2.¹⁰⁸ The seasonality index of nitrate was defined as the range of nitrate concentration in one grid cell divided by the maximum range encountered in WOA13 at the Tara sampling stations. All parameters were co-located with the corresponding stations and extracted at the month corresponding to the Tara sampling. To compensate for missing physicochemical samples in the *Tara in situ* dataset, climatological data (WOA) were favored. For details on the environmental niches, see Methods S1, Supplemental methods, Related to the STAR Methods.

Cosmopolitan score

Using metagenomes from the Station subset 1 (n = 757), MAGs and SAGs were assigned a “cosmopolitan score” based on their detection across 119 stations. For details on metagenomic subsets, see Methods S1, Supplemental methods, Related to the STAR Methods.

A database of manually curated DNA-dependent RNA polymerase genes

A eukaryotic dataset¹⁰⁹ was used to build HMM profiles for the two largest subunits of the DNA-dependent RNA polymerase (RNAP-a and RNAP-b). These two HMM profiles were incorporated within the *anvi'o* framework to identify RNAP-a and RNAP-b genes (Prodigal⁸⁷ annotation) in the MAGs and SAGs and METdb transcriptomes. Alignments, phylogenetic trees and blast results were used to organize and manually curate those genes. Finally, we removed sequences shorter than 200 amino-acids, providing a final collection of DNA-dependent RNA polymerase genes for the MAGs and SAGs ($n = 2,150$) and METdb ($n = 2,032$) with no duplicates. For details on this protocol, see [Methods S1](#), [Supplemental methods](#), Related to the [STAR Methods](#).

Novelty score for the DNA-dependent RNA polymerase genes

We compared both the RNA-Pol A and RNA-Pol B peptides sequences identified in MAGs and SAGs and MetDB to the nr database (retrieved on October 25, 2019) using *blastp*, as implemented in *blast+*¹¹⁰ v.2.10.0 (e-value of $1e^{-10}$). We kept the best hit and considered it as the closest sequence present in the public database. For each MAG and SAG, we computed the average percent identity across RNA polymerase genes (up to six genes) and defined the novelty score by subtracting this number from 100. For example, with an average percent identity of 64%, the novelty score would be 36%.

Phylogenetic analyses of MAGs and SAGs

The protein sequences included for the phylogenetic analyses (either the **DNA-dependent RNA polymerase genes** we recovered manually or the **BUSCO set of 255 eukaryotic single-copy core gene markers** we recovered automatically from the ~ 10 million protein coding genes) were aligned with MAFFT¹¹¹ v.7.64 and the FFT-NS-i algorithm with default parameters. Sites with more than 50% of gaps were trimmed using Galign v0.3.0-alpha5 (<http://www.github.com/evolbioinfo/goalign>). The phylogenetic trees were reconstructed with IQ-TREE¹¹² v1.6.12, and the model of evolution was estimated with the ModelFinder¹¹³ Plus option: for the concatenated tree, the LG + F + R10 model was selected. Supports were computed from 1,000 replicates for the Shimodaira-Hasegawa (SH)-like approximation likelihood ratio (aLRT)¹¹⁴ and ultrafast bootstrap approximation (UFBoot).¹¹⁵ As per IQ-TREE manual, we deemed the supports good when SH-aLRT $\geq 80\%$ and UFBoot $\geq 95\%$. *Anvi'o* v.6.1 was used to visualize and root the phylogenetic trees.

EggNOG functional inference of MAGs and SAGs

We performed the functional annotation of protein-coding genes using the EggNog-mapper^{58,59} v2.0.0 and the EggNog5 database.⁵⁷ We used Diamond¹¹⁶ v0.9.25 to align proteins to the database. We refined the functional annotations by selecting the orthologous group within the lowest taxonomic level predicted by EggNog-mapper.

Eukaryotic MAGs and SAGs integration in the AGNOSTOS-DB

We used the AGNOSTOS workflow to integrate the protein coding genes predicted from the MAGs and SAGs into a variant of the AGNOSTOS-DB that contains 1,829 metagenomes from the marine and human microbiomes, 28,941 archaeal and bacterial genomes from the Genome Taxonomy Database (GTDB) and 3,243 nucleocytoplasmic large DNA viruses (NCLDV) metagenome assembled genomes (MAGs).⁶⁴

AGNOSTOS functional aggregation inference

AGNOSTOS partitioned protein coding genes from the MAGs and SAGs in groups connected by remote homologies, and categorized those groups as members of the known or unknown coding sequence space based on the workflow described in Vanni et al. 2020.⁶⁴ To combine the results from AGNOSTOS and the EggNOG classification we identified those groups of genes in the known space that contain genes annotated with an EggNOG and we inferred a consensus annotation using a quorum majority voting approach. AGNOSTOS produces groups of genes with low functional entropy in terms of EggNOG annotations as shown in Vanni et al. 2020⁶⁴ allowing us to combine both sources of information. We merged the groups of genes that shared the same consensus EggNOG annotations and we integrated them with the rest of AGNOSTOS groups of genes, mostly representing the unknown coding sequence space. Finally, we excluded groups of genes occurring in less than 2% of the MAGs and SAGs.

Functional clustering of MAGs and SAGs

We used *anvi'o* to cluster MAGs and SAGs as a function of their functional profile (Euclidean distance with ward's linkage), and the *anvi'o* interactive interface to visualize the hierarchical clustering in the context of complementary information.

QUANTIFICATION AND STATISTICAL ANALYSIS

Differential occurrence of functions

We performed a Welch's ANOVA test followed by a Games-Howell test for significant ANOVA comparisons to identify EggNOG functions occurring differentially between functional groups of MAGs and SAGs. All statistics were generated in R 3.5.3. Results are available in the [Table S6](#).

Supplemental information

**Functional repertoire convergence of distantly
related eukaryotic plankton lineages
abundant in the sunlit ocean**

Tom O. Delmont, Morgan Gaia, Damien D. Hinsinger, Paul Frémont, Chiara Vanni, Antonio Fernandez-Guerra, A. Murat Eren, Artem Kourlaiev, Leo d'Agata, Quentin Clayssen, Emilie Villar, Karine Labadie, Corinne Cruaud, Julie Poulain, Corinne Da Silva, Marc Wessner, Benjamin Noel, Jean-Marc Aury, Tara Oceans Coordinators, Colombar de Vargas, Chris Bowler, Eric Karsenti, Eric Pelletier, Patrick Wincker, and Olivier Jaillon

Supplemental figures

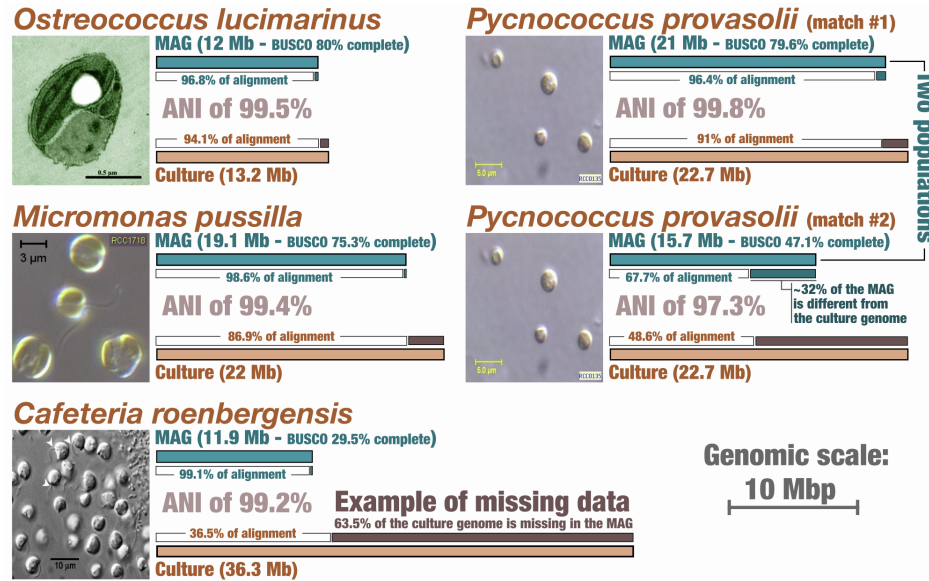


Figure S1. Genomic comparison of *Tara Oceans* MAGs and genomes from culture, Related to Figure 2. The figure summarizes the Average Nucleotide Identity (ANI) and percentage of genomic alignment for five matches between a MAG and a standard culture genome.

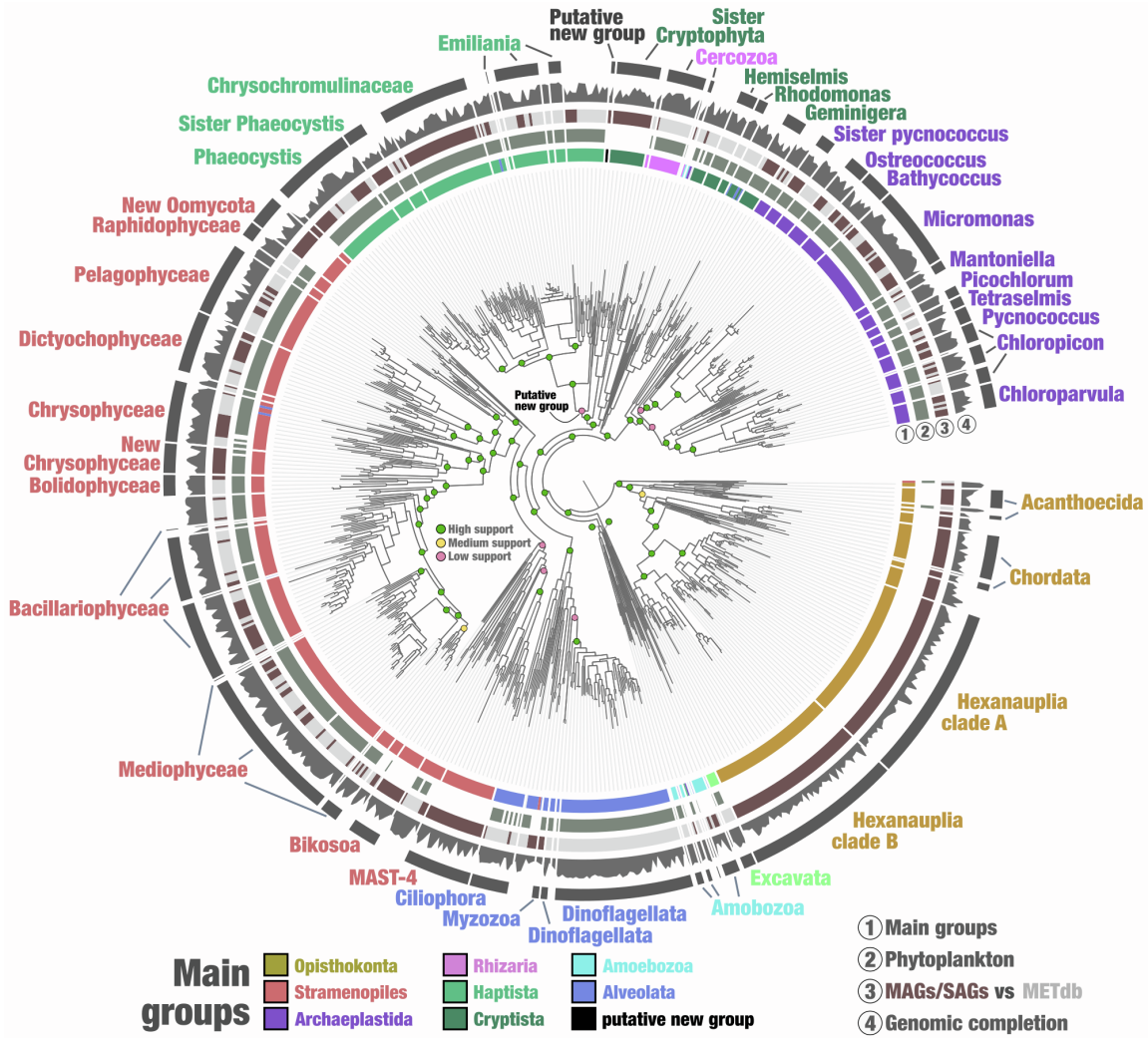


Figure S2. Phylogenomic analysis of the protein sequences of 255 BUSCO genes markers from eukaryotic plankton, Related to Figure 2. The maximum-likelihood phylogenomic tree of the BUSCO gene markers (255 genes) included *Tara* Oceans MAGs and METdb transcriptomes (minimum of 25% of completion) and was generated using a total of 19,785 sites in the alignment and LG+F+R10 model; Opisthokonta was used as the outgroup. The tree was decorated with additional layers using the *anvi'o* interface. Branches and names in red correspond to lineages lacking representatives in METdb.

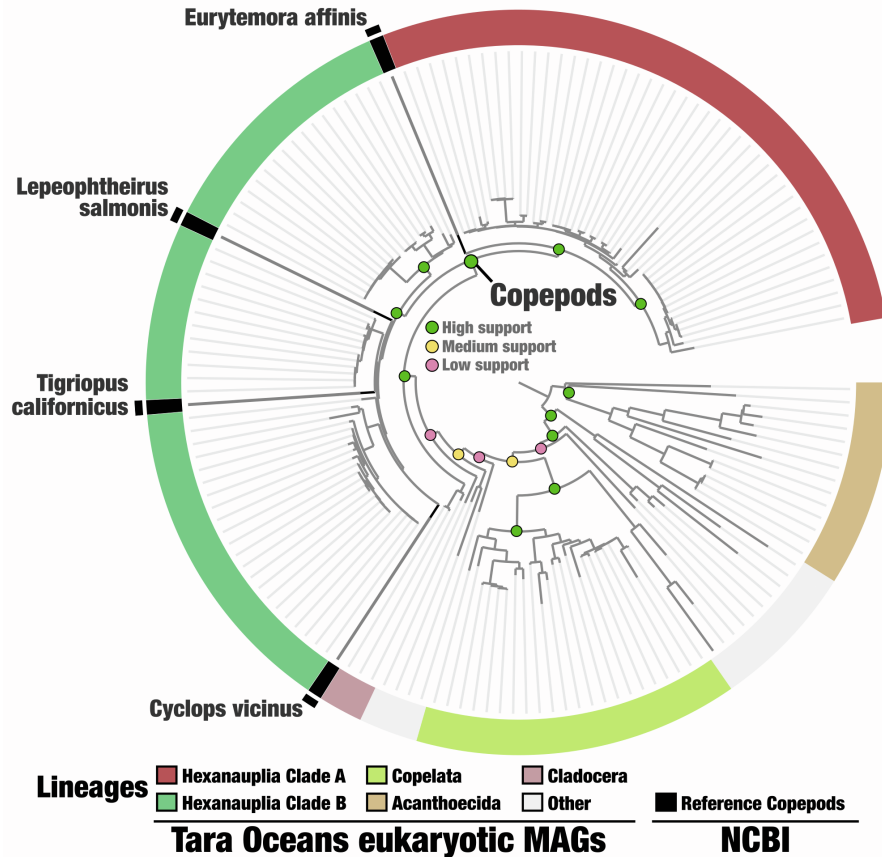


Figure S3: Phylogenetic analysis of concatenated DNA-dependent RNA polymerase II protein sequences from Opisthokonta MAGs and four copepod species, Related to Figure 2. The maximum-likelihood phylogenetic tree of the concatenated two largest subunits of the DNA-dependent RNA polymerases II (two genes) included *Tara* Oceans MAGs and reference copepod genomes (source: NCBI) and was generated using a total of 2,112 sites in the alignment and LG+R4 model (determined by ModelFinder); Acanthoecida were used as the outgroup. Supports for selected clades are displayed. Phylogenetic supports were considered high (aLRT \geq 80 and UFBoot \geq 95), medium (aLRT \geq 80 or UFBoot \geq 95) or low (aLRT $<$ 80 and UFBoot $<$ 95) (see Methods).

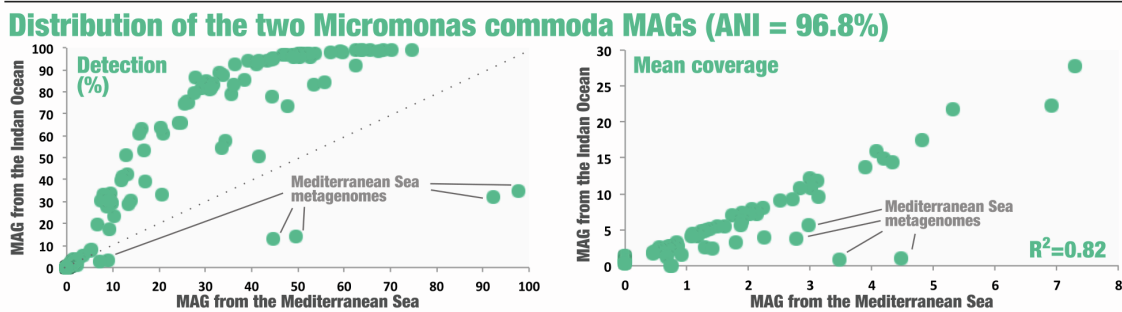
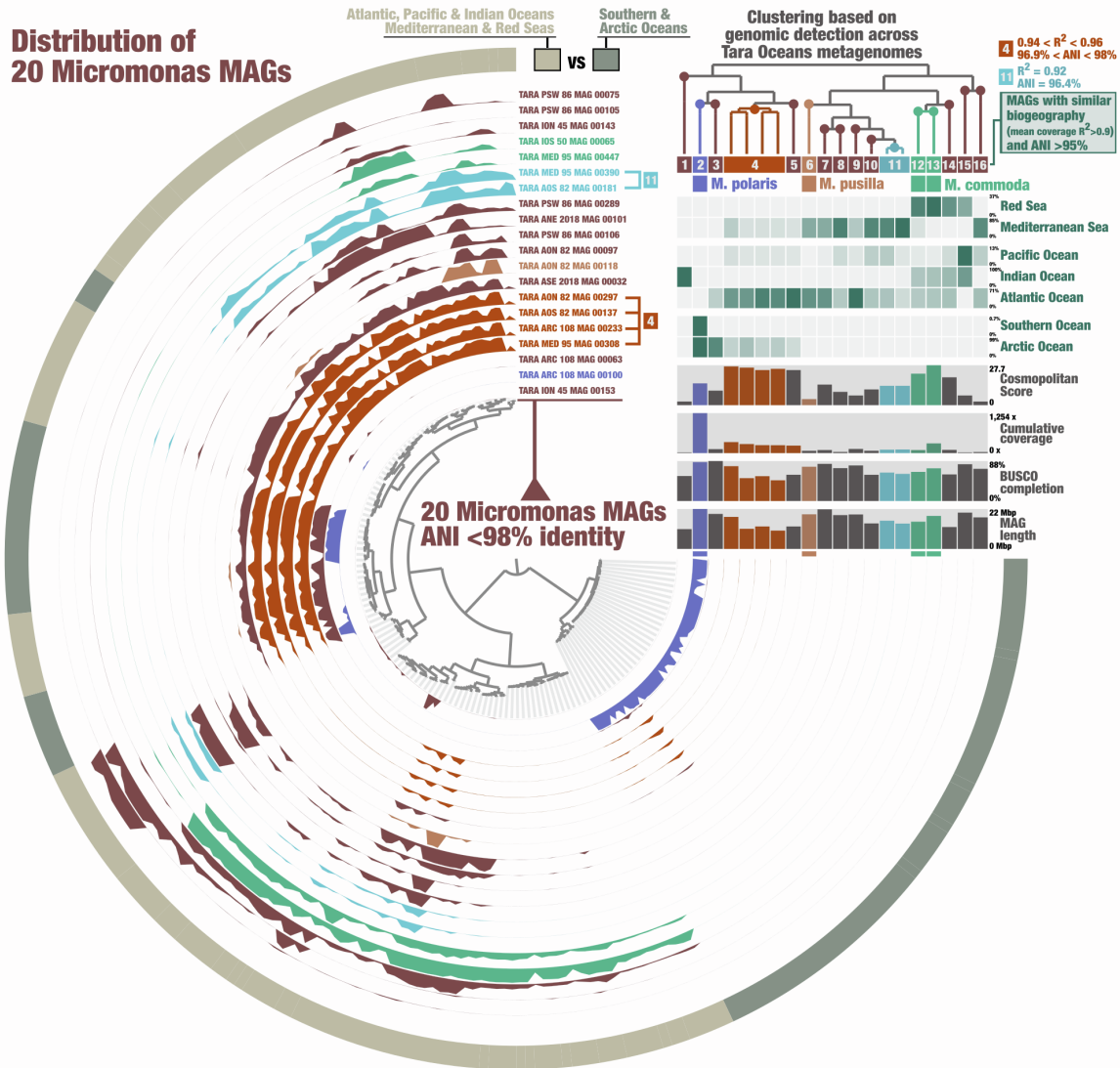


Figure S4: Biogeography of *Micromonas* populations, Related to Figure 2. Top panel displays the detection of 20 *Micromonas* MAGs across 258 *Tara* Oceans metagenomes for which at least one MAG was detected. The inner tree organizes the metagenomes as a function of the detection signal, and the tree on the top right corner organizes the MAGs based on the same signal. Thus, MAGs are organized based on similarities in their biogeography. MAGs with a coefficient of determination (R^2) > 0.9 for the mean coverage values across metagenomes and average nucleotide identity > 95% were linked to the same population Id. Populations “4” and “11” are represented by 4 MAGs and 2 MAGs, respectively. Bottom panel displays the detection (horizontal coverage) and mean coverage of two MAGs affiliated to *Micromonas commoda* across 939 *Tara* Oceans metagenomes.

Distribution of 11 Chloropicon MAGs

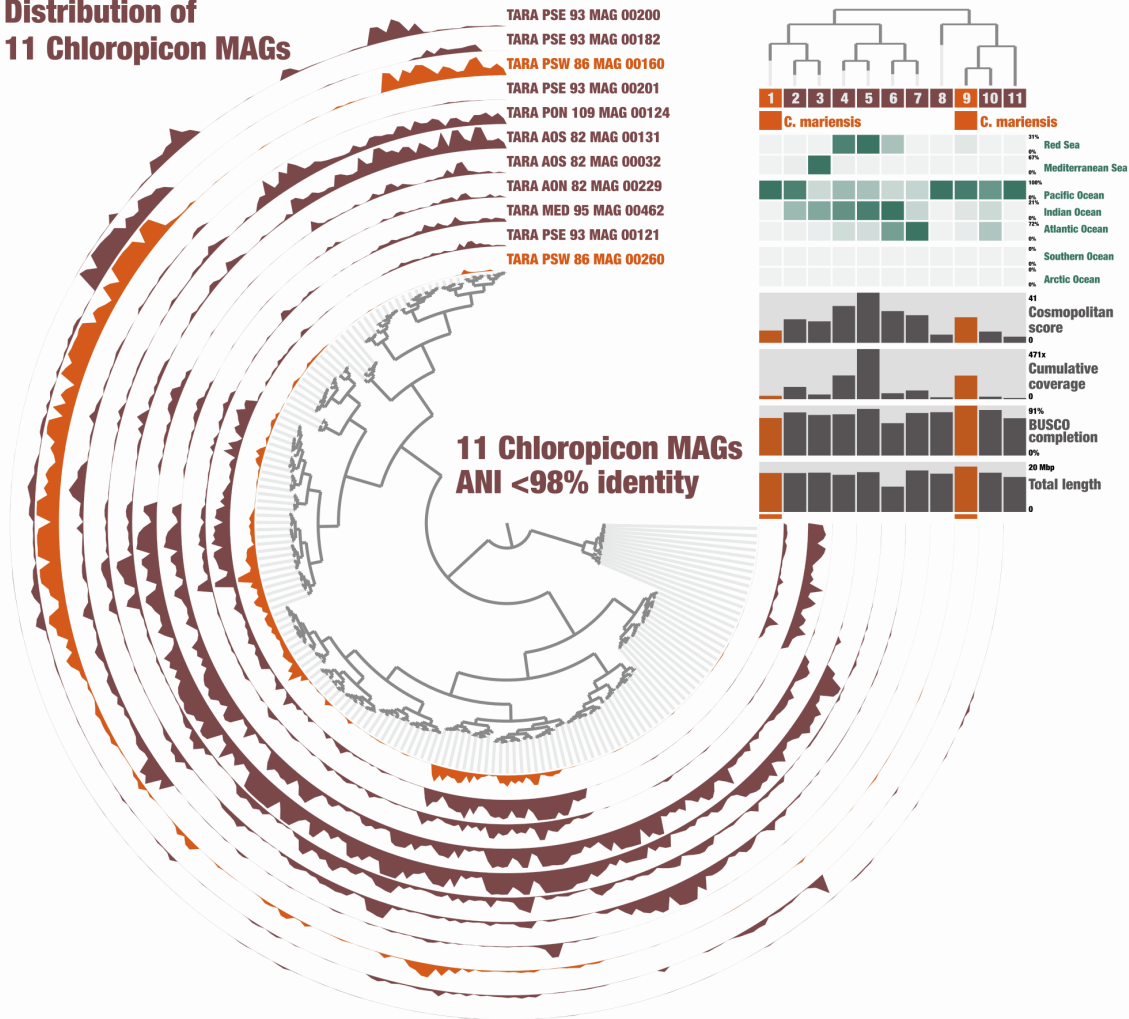


Figure S5: Biogeography of Chloropicon populations, Related to Figure 2. The figure displays the detection of 11 Chloropicon MAGs across 323 *Tara* Oceans metagenomes for which at least one MAG was detected. The inner tree organizes the metagenomes as a function of the detection signal, and the tree on the top right corner organizes the MAGs based on the same signal. Thus, MAGs are organized based on similarities in their biogeography. There were no MAGs with a coefficient of determination (R^2) > 0.9 for the mean coverage values across metagenomes and average nucleotide identity >95%. Thus, each MAG was linked to a distinct population Id.

Distribution of 8 Bathycoccus MAGs

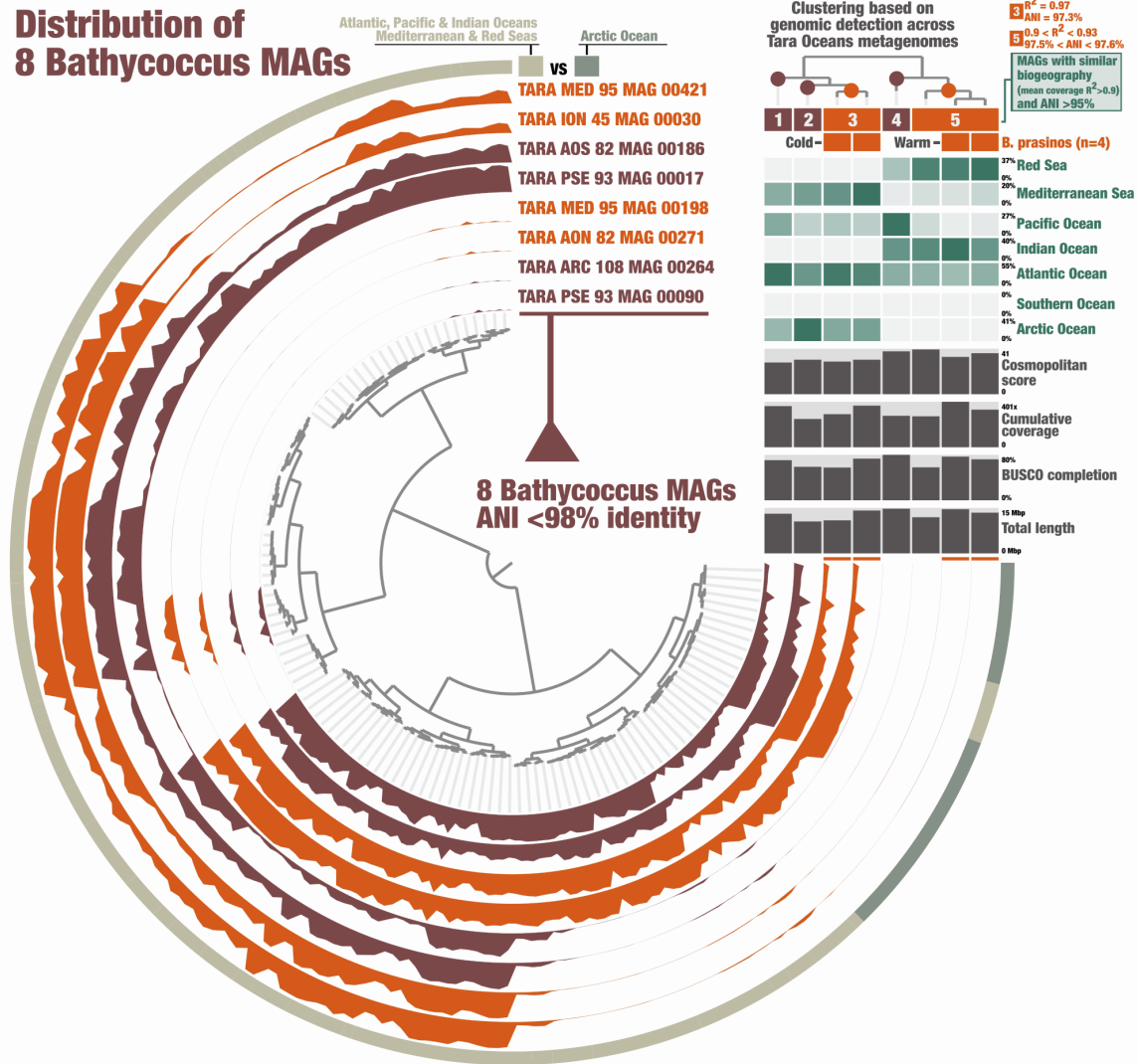


Figure S6: Biogeography of Bathycoccus populations, Related to Figure 2. The figure displays the detection of 8 Bathycoccus MAGs across 231 Tara Oceans metagenomes for which at least one MAG was detected. The inner tree organizes the metagenomes as a function of the detection signal, and the tree on the top right corner organizes the MAGs based on the same signal. Thus, MAGs are organized based on similarities in their biogeography. MAGs with a coefficient of determination (R^2) > 0.9 for the mean coverage values across metagenomes and average nucleotide identity >95% were linked to the same population Id. Populations “3” and “5” are represented by 2 MAGs and 3 MAGs, respectively.

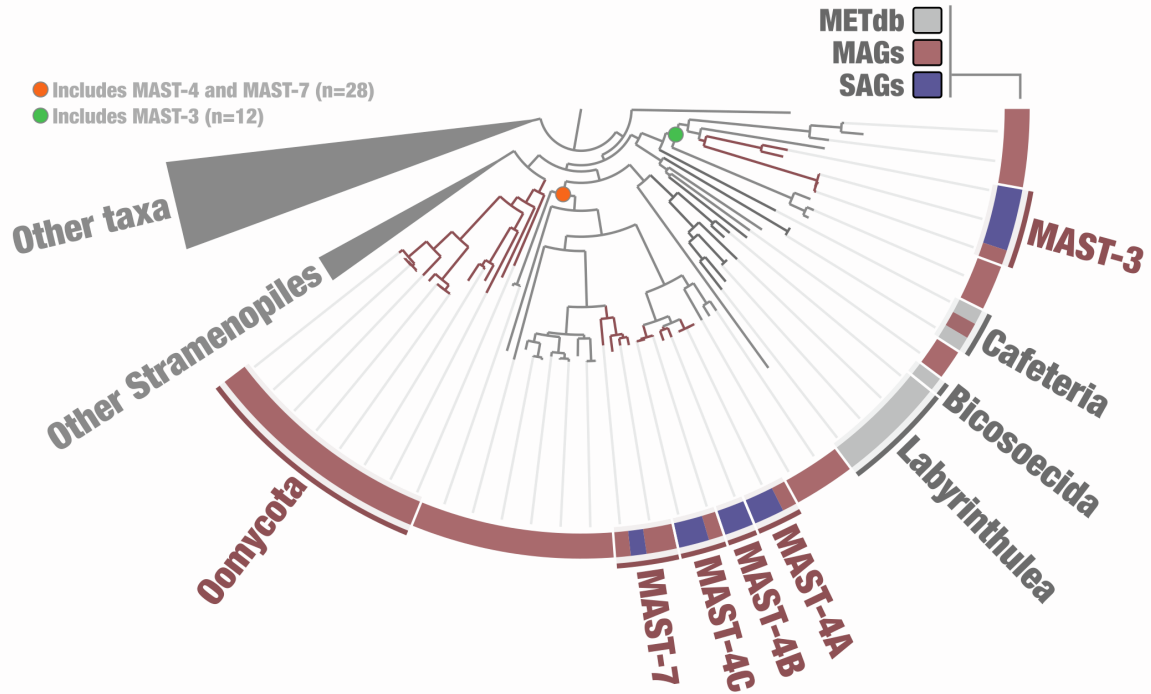


Figure S7: Phylogenetic analysis of concatenated DNA-dependent RNA polymerase protein sequences from eukaryotic plankton, Related to Figure 2. The maximum-likelihood phylogenetic tree of the concatenated two largest subunits from the three DNA-dependent RNA polymerases (six genes in total) included *Tara* Oceans MAGs and SAGs along with METdb transcriptomes and was generated using a total of 7,243 sites in the alignment and LG+F+R10 model; Here large groups were collapsed to better visualize the diversity of MAST lineages. SAGs were affiliated to taxonomic lineages based on 18S rRNA gene analyses.

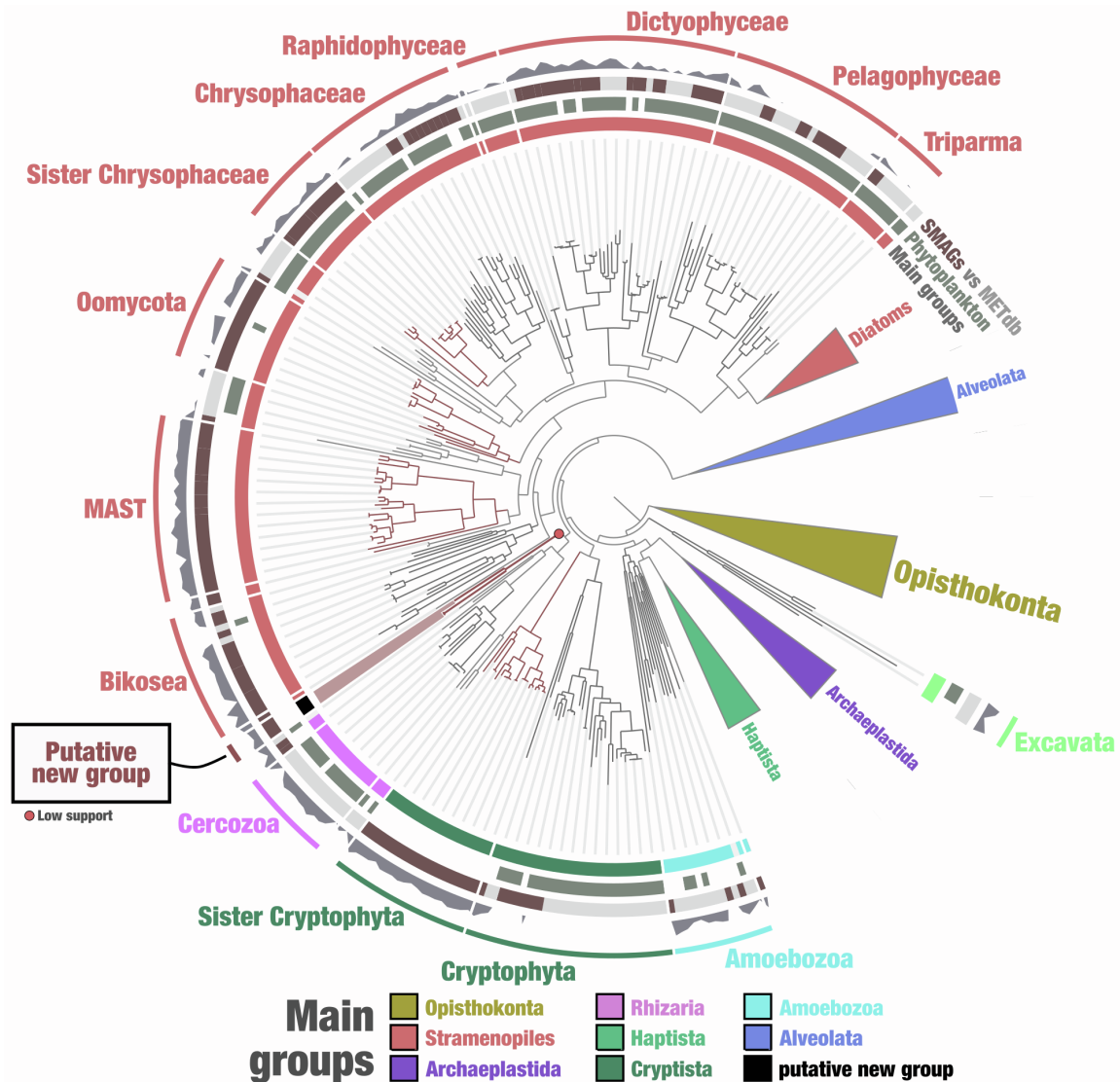


Figure S8: Phylogenetic analysis of concatenated DNA-dependent RNA polymerase protein sequences from eukaryotic plankton, Related to Figure 2. The maximum-likelihood phylogenetic tree of the concatenated two largest subunits from the three DNA-dependent RNA polymerases (six genes in total) included *Tara* Oceans MAGs and SAGs along with METdb transcriptomes and was generated using a total of 7,243 sites in the alignment and LG+F+R10 model; Opisthokonta was used as the outgroup. Support for the putative new group is displayed. Phylogenetic supports were considered high (aLRT \geq 80 and UFBoot \geq 95), medium (aLRT \geq 80 or UFBoot \geq 95) or low (aLRT $<$ 80 and UFBoot $<$ 95) (see Methods).

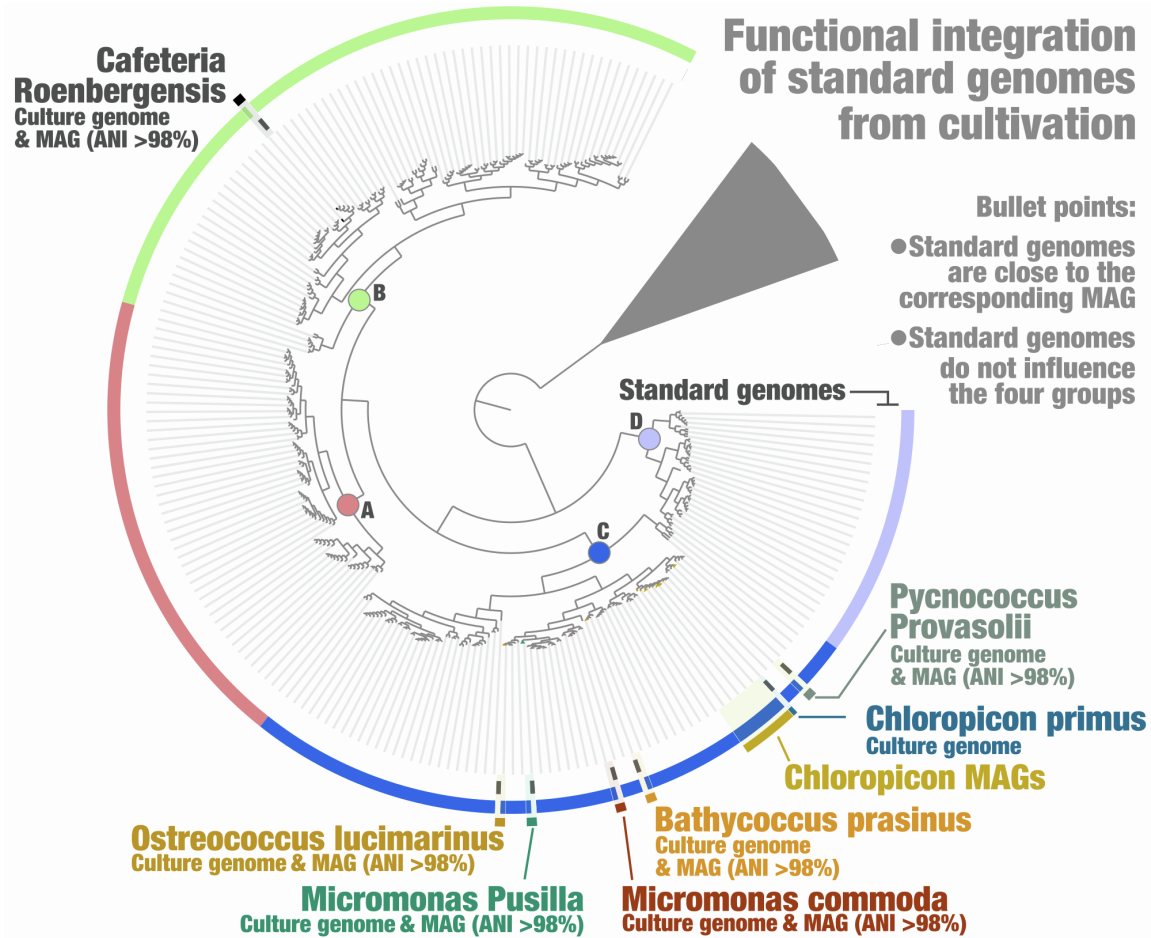


Figure S9: Functional clustering based on MAGs, SAGs and seven culture genomes, Related to Figure 3. The figure displays a hierarchical clustering (Euclidean distance with Ward's linkage) of MAGs, SAGs and seven closely related standard culture genomes (predicted proteins were imported from NCBI) based on the occurrence of the functions identified with EggNOG, rooted with small animals (Chordata, Crustacea and copepods) and decorated with layers of information using the anvio interactive interface. As for the previous analyses, removed from the analyses were Ciliophora MAGs (gene calling is problematic for this lineage), and functions occurring more than 500 times in the gigabase-scale MAG and linked to retrotransposons connecting otherwise unrelated MAGs and SAGs.

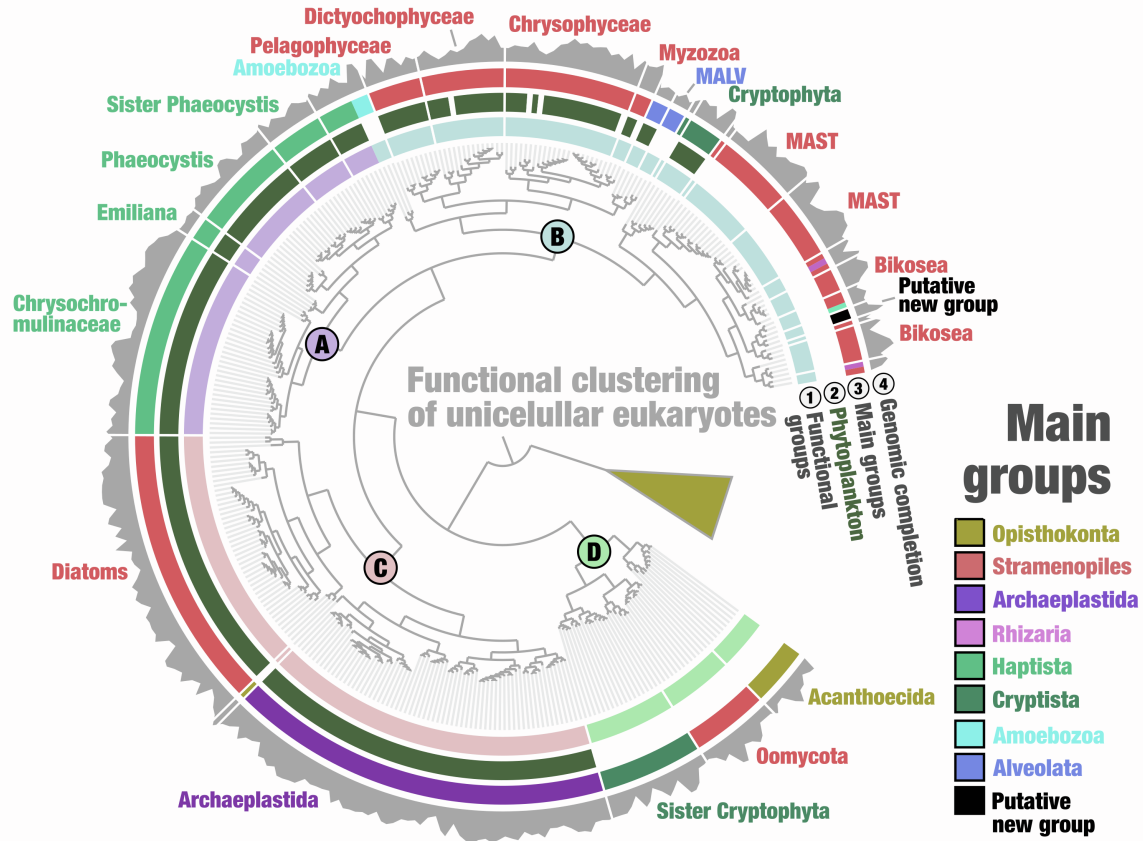


Figure S10: Functional clustering based on MAGs and SAGs with high completion estimates, Related to Figure 3. The figure displays a hierarchical clustering (Euclidean distance with Ward's linkage) of 483 MAGs and SAGs >25% complete (BUSCO estimation) based on the occurrence of 27,415 functions identified with EggNOG, rooted with small animals (Chordata, Crustacea and copepods) and decorated with layers of information using the anvio interactive interface. As for the previous analyses, removed from the analyses were Ciliophora MAGs (gene calling is problematic for this lineage), and functions occurring more than 500 times in the gigabase-scale MAG and linked to retrotransposons connecting otherwise unrelated MAGs and SAGs.

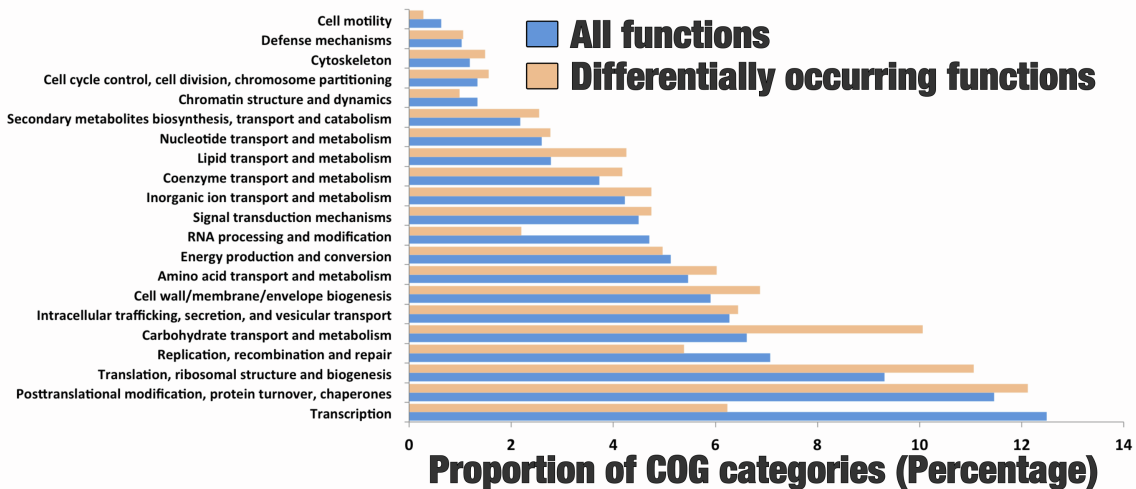


Figure S11. Relative proportion of known COG categories in annotated functions versus those that were significantly differentially occurring between the four functional groups, Related to Figure 3.

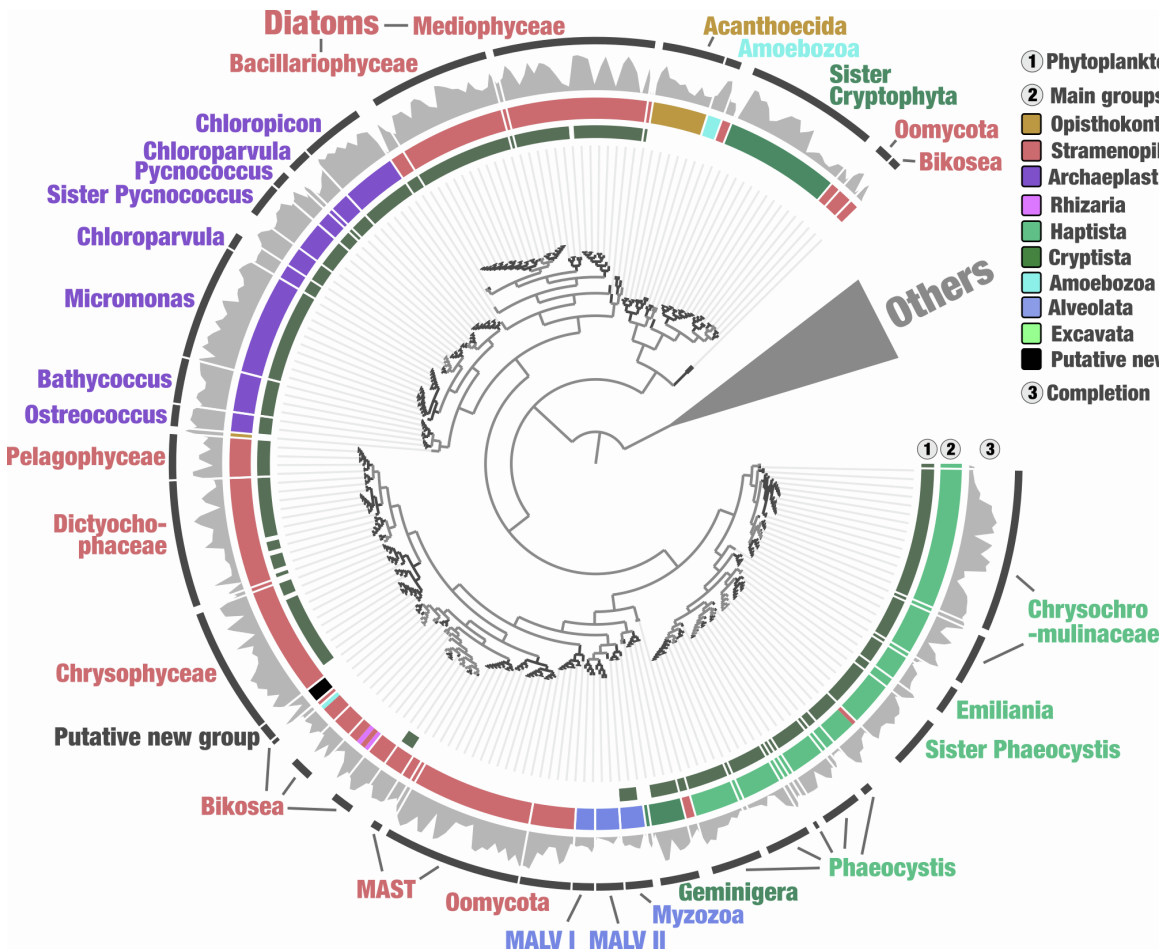


Figure S12. Functional landscape of unicellular eukaryotes in the sunlit ocean by combining EggNOG and Agnostos for gene processing, Related to Figure 3. The figure displays a hierarchical clustering (Euclidean distance with Ward's linkage) of 681 MAGs and SAGs based on the occurrence of ~39,705 groups of genes (total of 5,178,829 genes) identified by combining EggNOG⁵⁸⁻⁶⁰ with Agnostos⁶⁵, rooted with MAGs dominated by small animals (Chordata, Crustacea and copepods) and decorated with layers of information using the anvio interactive interface. Removed from the analysis were Ciliophora MAGs (gene calling is problematic for this lineage), and functions occurring more than 1,000 times in the gigabase-scale MAG and linked to retrotransposons connecting otherwise unrelated MAGs and SAGs, or occurring in less than 2% of the MAGs and SAGs.

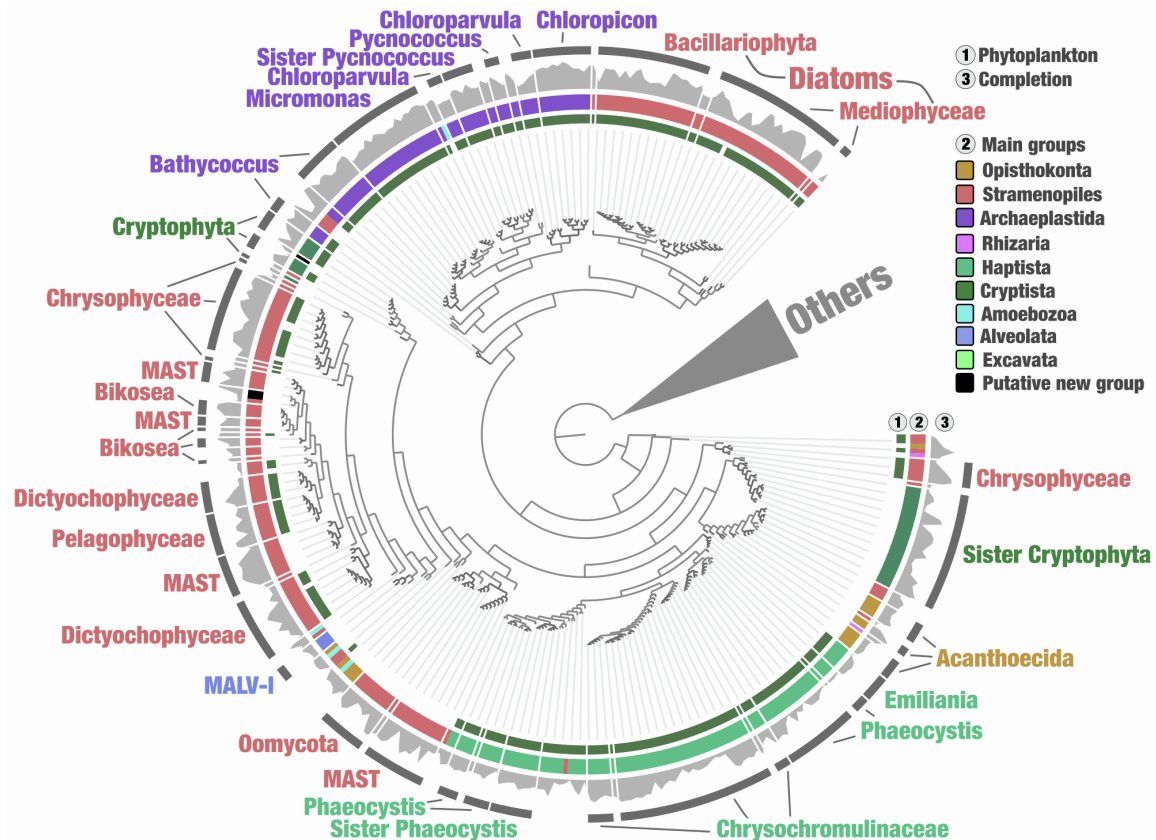


Figure S13. The genomic unknown functional landscape of unicellular eukaryotes in the sunlit ocean, Related to Figure 3. The figure displays a hierarchical clustering (Euclidean distance with Ward's linkage) of 681 MAGs and SAGs based on the occurrence of ~28,000 gene clusters of unknown function (total of 1.3 million genes) identified by solely with Agnostos⁶⁵ (environmental unknowns plus genomic unknowns), rooted with MAGs dominated by small animals (Chordata, Crustacea and copepods) and decorated with layers of information using the anvio interactive interface. Removed from the analysis were Ciliophora MAGs (gene calling is problematic for this lineage), and functions occurring more than 1,000 times in the gigabase-scale MAG and linked to retrotransposons connecting otherwise unrelated MAGs and SAGs, or occurring in less than 2% of the MAGs and SAGs.

Supplemental tables

Table S1.

Table S2.

Table S3.

Table S4.

Table S5.

Table S6.

Table S7.

Table S8.

Table S9.

Methods S1: supplemental methods, related to the STAR Methods.

#1: Genome-resolved metagenomics with anvi'o.

A set of single copy core genes to identify eukaryotic MAGs

As initially outlined in a blog post published at the beginning of this project to benefit others¹, we have defined a set of 83 single copy core genes from BUSCO² compatible with the gene calling workflow of anvi'o³ to best estimate the completion of eukaryotic metagenome-assembled genomes (MAGs). Figure S14 describes the efficacy of this collection to estimate completion of MAGs from *Micromonas* and *Ostreococcus*. Note that those estimates are only initial, since this stage of the workflow uses a gene calling (Prodigal⁴) that is not optimal for eukaryotes. However, the results are sufficiently robust to effectively guide the manual binning and curation of eukaryotic MAGs without the need to first identify eukaryotic contigs in the assembly output. While the identification of eukaryotic contigs prior to binning as been benchmarked by the group of Jill banfield⁵, false positives and false negatives associated with this critical step can be problematic and are entirely avoided in our workflow. We found that binning metagenomes containing multiple domains of life can be done smoothly within anvi'o, as long as proper single copy core gene collections are used to efficiently affiliate MAGs to Bacteria, Archaea and Eukarya. Note that this dedicated collection for eukaryotes is the main improvement within anvi'o compared to the workflow outlined for the characterization of ~1,000 bacterial and archaeal MAGs from small size fractions of TARA Oceans⁶. It is now an integral component of the anvi'o metagenomic flow used by a growing number of scientists interested in genome-resolved metagenomics.

Preliminary results using the single copy core gene collection "BUSCO_83_Protista"

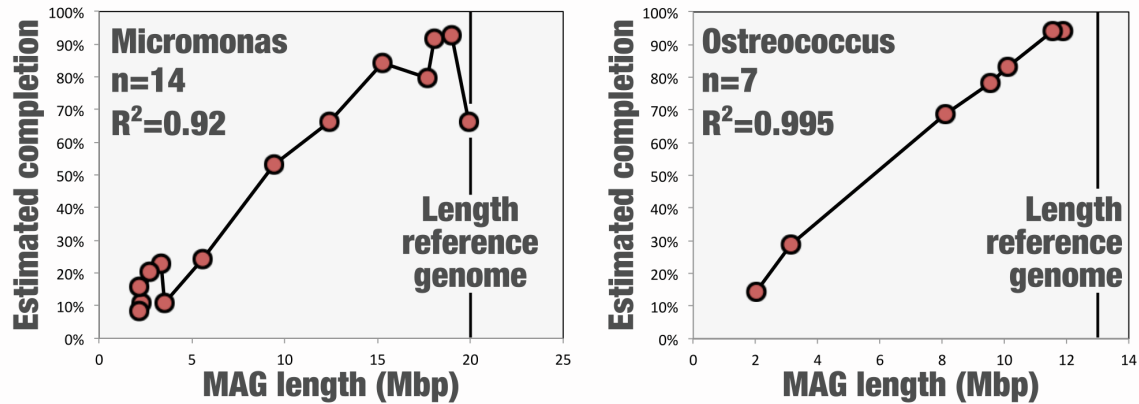


Figure S14: Completion estimates for *Micromonas* and *Ostreococcus* MAGs using a set of 83 BUSCO single copy core genes, as a function of the length of the MAGs.

A summary of the workflow to bin and curate eukaryotic MAGs

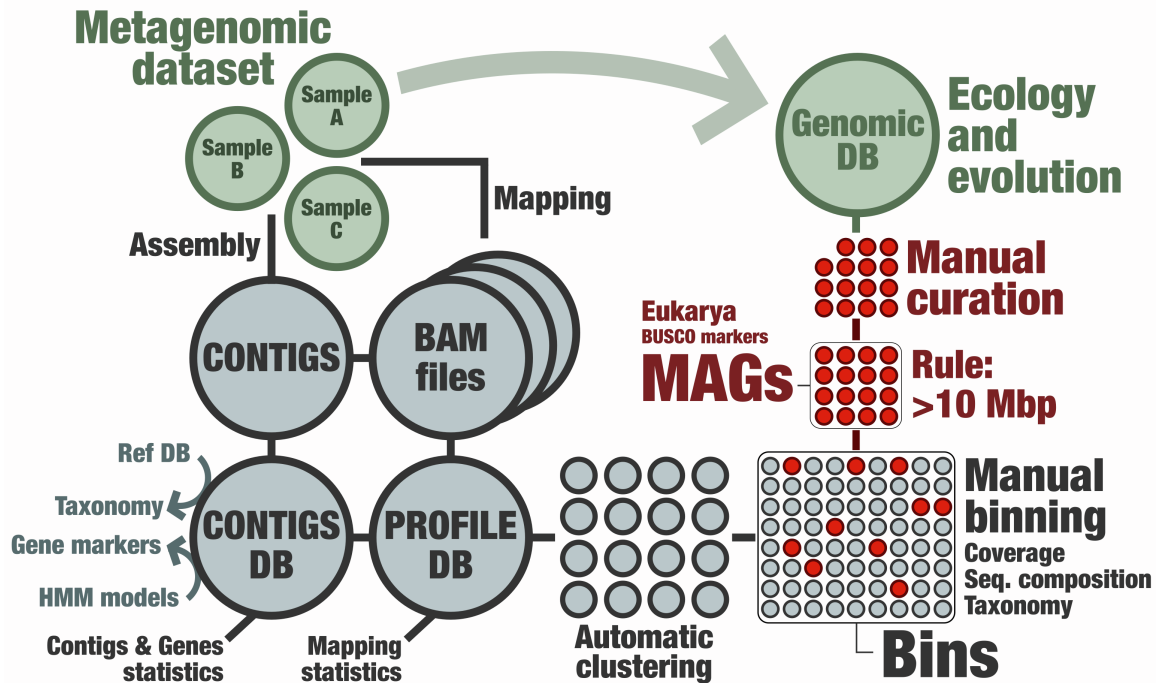


Figure S15: The manual genome-resolved metagenomic framework of *anvi'o* dedicated to the eukaryotes. This workflow is to be applied to each assembly outcome.

We followed the workflow outlined in the figure s15 for each of the 11 metagenomic co-assemblies outlined in the study (see Table S2). Briefly, we used the sequence composition of contigs and their differential coverage across metagenomes to perform a first automatic binning step with CONCOCT⁷ by constraining the number of created clusters (thereafter dubbed metabins) to a number substantially below the number of genomes in the assembly. This number ranged from 50 to 400 depending on the assembly volume. Note that CONCOCT is used because the interactive interface of *anvi'o* cannot work efficiently when loading >25k contigs.

For each metabin, we then used the anvi'o interactive interface to manually identify and curate eukaryotic MAGs. This step took about 10 months of manual work.

An holistic interactive interface now compatible with eukaryotes

Within the framework of our study, the anvi'o interactive interface took advantage of the sequence composition of contigs, their differential coverage across metagenomes, taxonomic signal using a reference database that includes METdb, and HMM models for single copy core gene collections (Bacteria, Archaea, Eukarya). When selecting a cluster of contigs corresponding to a MAG in the interface, anvi'o identified its domain affiliation in real time using random forest, and displayed its completion and redundancy values accordingly. This way, it was possible to focus on the eukaryotic MAGs within an assembly containing also many abundant bacterial and archaeal MAGs. In the figure S16, we provide the example of one metabin from the Mediterranean Sea metagenomic co-assembly (95 metagenomes) containing eukaryotic MAGs for *Ostreococcus* and *Micromonas* (left panel). In this simple example, we selected those two clusters in the interface, saved the collection, and subsequently manually curated them as presented here for *Ostreococcus* (right panel). This MAG exhibited a completion of 100% and a redundancy of 3%. One metagenome (most outer blue layer) was particularly useful in this particular case since the *Micromonas* MAG was more detected compared to the *Ostreococcus* MAG, allowing an effective binning outcome. Given the complexity of marine metagenomes, differential coverage across dozens of metagenomes strongly benefited to the outcome of our genome-resolved metagenomic survey.

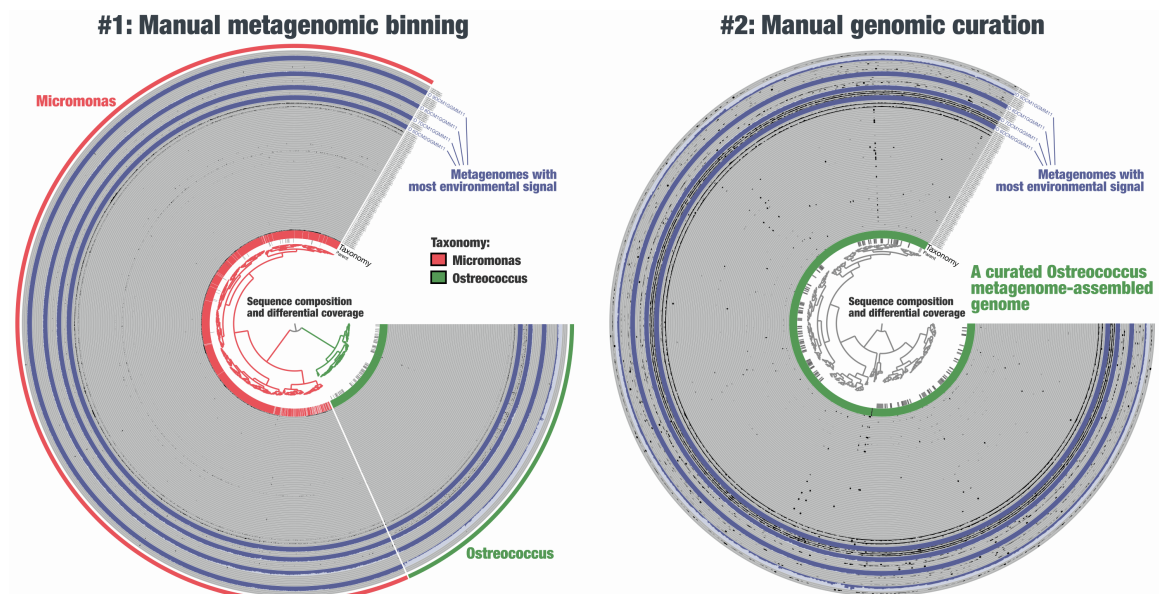


Figure S16: The anvi'o interactive interface to manually bin and curate eukaryotic MAGs. The left panel displays the detection of contigs from a single metabin across 95 metagenomes, alongside taxonomic signal. Clustering was done using sequence composition and differential coverage. Right panel displays the curated *Ostreococcus* MAGs identified from the left panel.

Example of environmental signal for a manually curated Ciliophora MAG

We provide an example of manually curated MAG (“TARA MED 95 MAG 00445”), for which environmental signal is described using both detection (horizontal coverage, left panel) and mean coverage (vertical coverage, right panel):

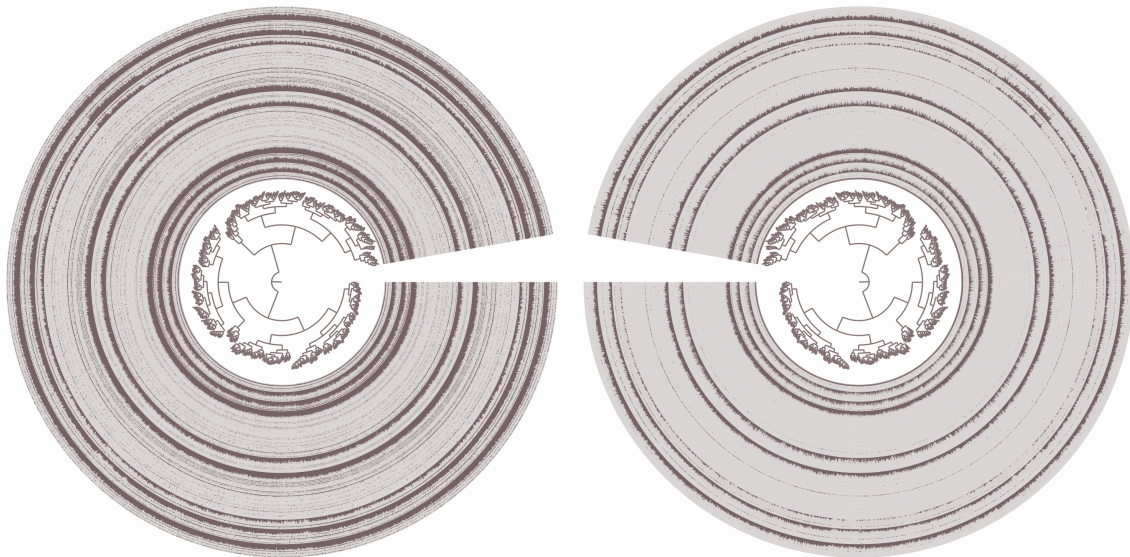


Figure S17: Example of a manually curated eukaryotic MAG as visualized in the *anvi'o* interactive. The selected MAG is named “TARA MED 95 MAG 00445”. It is affiliated to Ciliophora and contains 2,613 contigs for a length of 13.5 Mbp. Clustering of contigs was done using sequence composition alone. Then, the left and right panels respectively display the detection and mean coverage of contigs across the 95 *Tara* Oceans metagenomes, which were used to assess the quality of this MAG and others.

We can observe strong environmental signal coherence for the 2,614 contigs. The contigs correlated across the 95 metagenomes considered, with no particular outliers when it comes to sequence composition either. Critically, the coherence of environmental signal is supportive of the quality of the MAGs, which were all manually inspected and curated.

#2: Decontamination of single cell genomes with *anvi'o*.

Eukaryotic single cell genomes (SAGs) can be heavily contaminated due to a combination of factors during cell sorting, DNA extraction and amplification, and multiplex sequencing. Here, we slightly modified the *anvi'o* metagenomic workflow to effectively decontaminate marine eukaryotic SAGs, one by one. Briefly, we used the *anvi'o* interactive interface to manually curate eukaryotic SAGs by taking into consideration the sequence composition of contigs, their differential coverage across 100 most relevant metagenomes (i.e., those with highest mapping recruitment scores within the scope of TARA Oceans), taxonomic signal using a reference database that includes METdb, and HMM models for single copy core gene collections (Bacteria, Archaea, Eukarya). Note that compared to the metagenomic co-assemblies, the number of contigs under consideration was orders of magnitude

smaller. Since all contigs could be loaded in the interactive interface, there was no need to use the pre-clustering step with CONCOCT. However, CONCOCT could also be used here if some SAG assemblies include more than ~25k contigs.

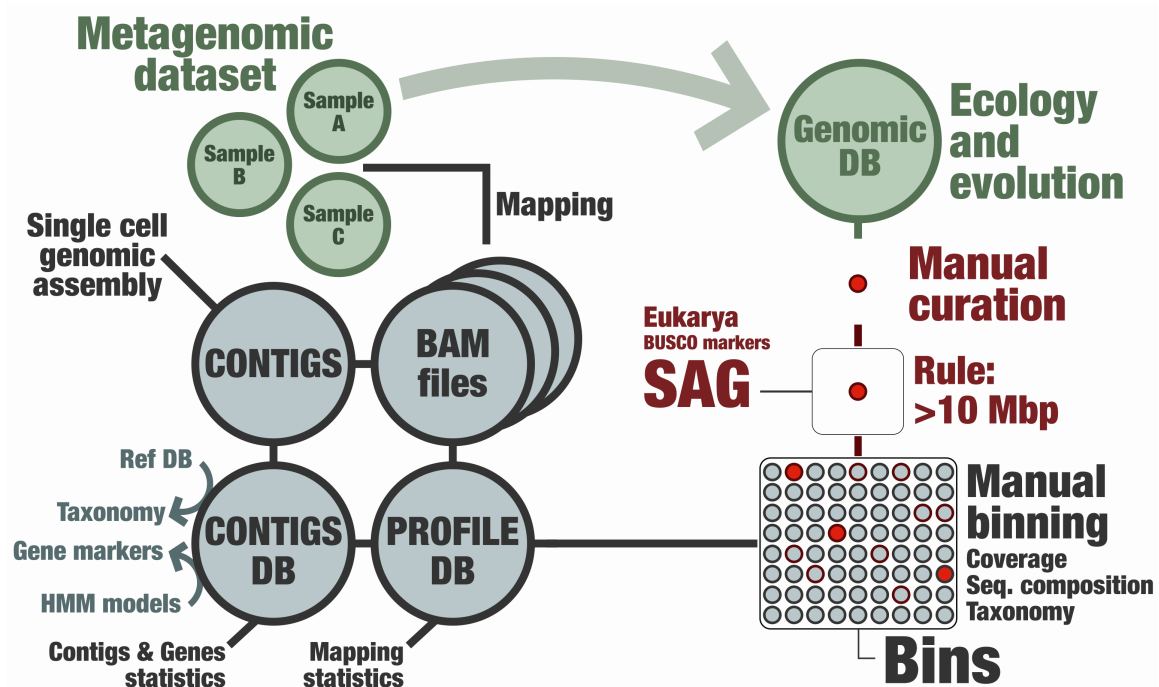


Figure S18: The manual metagenomic framework of anvi'o dedicated to the decontamination of SAGs. This workflow was applied to each SAG (co-)assembly outcome.

Figure S19 provides a striking example of heavily contaminated SAG we could effectively curate thanks to the clear differential coverage signal of contigs across 100 metagenomes. In this particular case, contamination seemed to have multiple origins, and a large number of contigs were removed. Overall, our manual curation of SAGs using a genome-resolved metagenomics workflow initially built for MAGs turned out to be highly valuable, leading in our study to the removal of more than one hundred thousand scaffolds for a total volume of 193.1 million nucleotides. This metagenomic-guided decontamination effort contributes to previous efforts characterizing eukaryotic SAGs from the same cell sorting material⁸⁻¹² and provides new guidelines for marine eukaryotic SAGs. We now recommend this approach for future efforts generating eukaryotic SAGs from the sunlit ocean. This is important, especially since SAGs could become a valuable asset in the near future to target lineages genome-resolved metagenomics failed to recover so far. It is especially the case of Dinoflagellates.

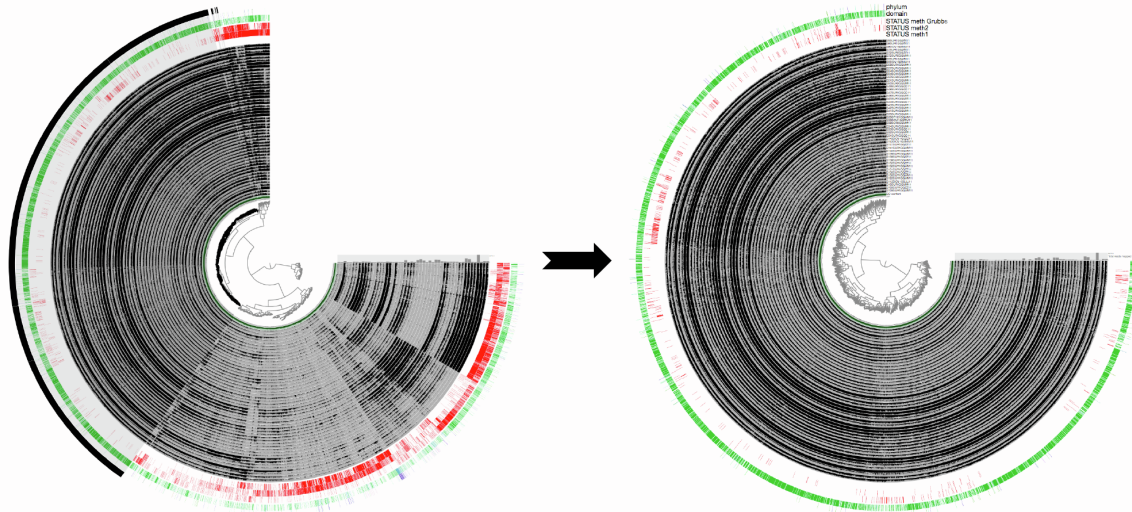


Figure S19: Example of the decontamination of TOSAG00-8. Left panel describes all contigs reconstructed from this SAG, organized based on sequence composition and differential coverage across 100 *Tara* Oceans metagenomes. The selection of contigs (outer layer) corresponds to our final curated SAG, displayed in the right panel, for which clustering is based on sequence composition alone.

#3: The METdb database for eukaryotic transcriptomes.

METdb is a curated database of transcriptomes from marine eukaryotic isolates that cover the MMETSP collection¹³ (new assemblies were performed, combining time points from the same culture in co-assemblies when available) as well as cultures from TARA Oceans. The associated manuscript is not yet published. However, the database is publically available and can be accessed at <http://metdb.sb-roscoff.fr/metdb/>.

#4: World map projections.

World Ocean Atlas data

Seven physicochemical parameters were used to define environmental niches: sea surface temperature (SST), salinity (Sal), dissolved silica (Si), nitrate (NO_3), phosphate (PO_4), iron (Fe), and a seasonality index of nitrate (SI NO_3). With the exception of Fe and SI NO_3 , these parameters were extracted from the gridded World Ocean Atlas 2013 (WOA13)²¹. Climatological Fe fields were provided by the biogeochemical model PISCES-v2²². The seasonality index of nitrate was defined as the range of nitrate concentration in one grid cell divided by the maximum range encountered in WOA13 at the Tara sampling stations. All parameters were co-located with the corresponding stations and extracted at the month corresponding to the Tara sampling. To compensate for missing physicochemical samples in the Tara *in situ* data set, climatological data (WOA) were favored. The correlation between *in situ* samples and corresponding values extracted from WOA were high:

R-squared values for the surface samples:

SST: 0.99, Sal: 0.86, Si: 0.89, NO₃: 0.85, PO₄: 0.90

R-squared values for the DCM samples:

SST: 0.97, Sal: 0.47, Si: 0.97, NO₃: 0.74, PO₄: 0.85

In the absence of corresponding WOA data, a search was done within 2° around the sampling location and values found within this square were averaged.

Nutrients, such as NO₃ and PO₄, displayed a strong collinearity when averaged over the global ocean (correlation of 0.95 in WOA13), which could complicate disentangling their respective contribution to niche definition. However, observations and experimental data allow distinguishing between limiting nutrients at regional scale characterized by specific plankton communities²³. The future projection of niches will yield spurious results when the present-day collinearity is not maintained^{24,25}. To this day, there is no evidence for large scale changes in global nutrient stoichiometry²⁶.

Earth System Models and bias correction

Outputs from six Earth system models were used to project environmental niches under greenhouse gas emission scenario RCP8.5²⁷:

Model	Reference
CESM1-BGC	Gent et al., 2011
GFDL-ESM2G	Dunne et al., 2013
GFDL-ESM2M	Dunne et al., 2013
HadGEM2-ES	Collins et al., 2011
IPSL-CM5A-LR	Dufresne et al., 2013
IPSL-CM5A-MR	Dufresne et al., 2013
MPI-ESM-LR	Giorgetta et al., 2013
MPI-ESM-MR	Giorgetta et al., 2013
NorESM1-ME	Bentsen et al., 2013

Table 1: Summary of Earth system models used to project environmental niches.

Environmental drivers were extracted for present day (2006-2015) and end of century (2090-2099) conditions for each model and the multi-model mean was computed. A bias correction method, the Cumulative Distribution Function transform, CDFt²⁸, was applied to adjust the distributions of SST, Sal, Si, NO₃ and PO₄ of the multi-model mean to the WOA database. CDFt is based on a quantile mapping (QM) approach to reduce the bias between modeled and observed data, while accounting for climate change. Therefore, CDFt does not rely on the stationary hypothesis and present and future distributions can be different. CDFt was applied on the global fields of the mean model simulations. By construction, CDFt preserved the ranks of the simulations to be corrected. Thus, the spatial structures of the model fields were preserved.

Environmental niches models: training, validation and projections

From the initial dataset of 713 SMAGs, we selected those present in at least 4 stations for environmental niche training, discarding just 58 of them. Four machine learning methods were applied to compute environmental niches for each of the 655 remaining SMAGs:

- (1) Gradient Boosting Machine (gbm)²⁹
- (2) Random Forest (rf)³⁰
- (3) Fully connected Neural Networks (nn)³¹
- (4) Generalized Additive Models (gam)³²

Hyper parameters of each technique (except gam) were optimized as followed:

- (1) For gbm, the interaction depth (1, 3 and 5), learning rate (0.01, 0.001) and the minimum number of observations in a tree node (1 to 10)
- (2) For rf, the number of trees (100 to 900 with step 200 and 1000 to 9000 with step 2000) and the number of parameters used for each tree (1 to 8)
- (3) For nn, the number of layers of the network (1 to 10) and the decay (1.10-4 to 9.10-4 and 1.10-5 to 9.10-5)
- (4) For gam the number of splines was set to 3.

R packages gbm (2.1.3), randomForest (4.6.14), mgcv (1.8.16) and nnet (7.3.12) were used for gbm, rf, nn and gam models.

To define the best combination of hyper parameters for each model, we perform 30 random cross-validations by training the model on 75% of the dataset randomly sampled and by calculating the Area Under the Curve⁵¹ (AUC) on the 25% remaining points of the dataset. The best combination of hyper parameters is the one for which the mean AUC over the 30 cross-validation is the highest. A model is considered valid if at least 3 out of the 4 techniques have a mean AUC superior to 0.65, which is the case for 374 out of the 655 SMAGs (57%). Final models are trained on the full dataset and only the techniques that have a mean AUC higher than 0.65 are considered to make the projections. The majority (286) of the 374 validated niches is validated by all four models and 88 by only 3 models. Relative influences of each parameter in defining environmental niches are calculated using the feature_importance function from the DALEX R package³³ for all four statistical methods. For model training and projections, physicochemical variables are scaled to have a mean of 0 and a variance of 1. For this scaling, the mean and standard deviation of each WOA13 variable (+ PISCES-v2 Fe) co-localized with Tara stations with a value available is used. This standardization procedure allows for better performance of models. Finally, as statistical models often disagree we use the ensemble model approach for global-scale projections of niches³⁴ i.e. the mean projections of the validated machine learning techniques.

Environmental niches models at Tara Oceans stations

Here we describe the performances of the statistical models on biogeochemical model projections at locations of the training set (*i.e.* the Tara stations). Our models are only presence/absence models so they project probabilities of presence (not relative abundances) of a given MAG at each gridded point of the ocean based on environmental parameters. The figure S20 presents the specificity in function of the sensitivity for each model (*i.e.* each point is a MAG) calculated on the set of *Tara* stations for biogeochemical projections and for two threshold of presence detection ($p>0.5$ and $p>0.3$). The specificity captures the ability of the model to correctly detect absences while the sensitivity captures its capability to detect presences. Details on model computation and validation are in the supplementary material.

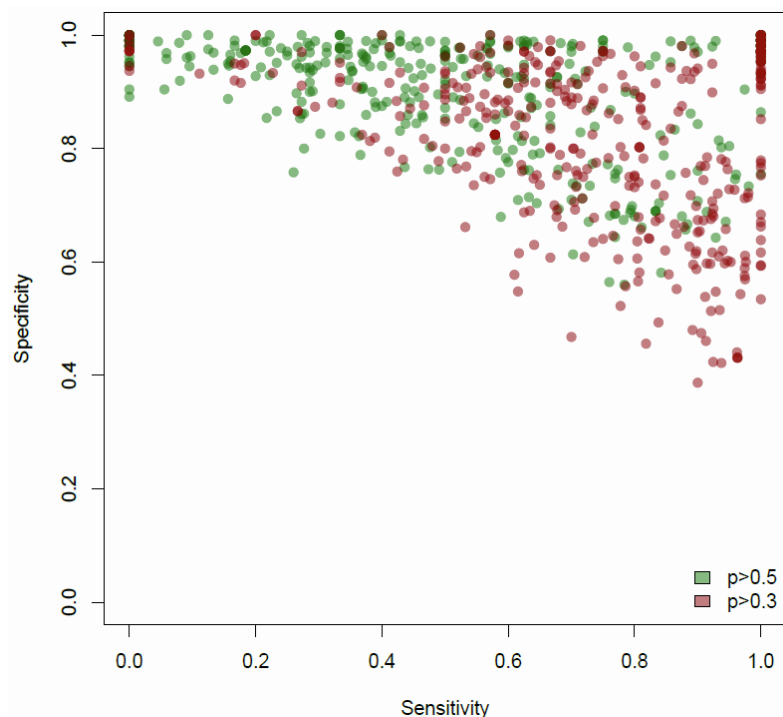


Figure S20: Statistical niches model performances for each MAG on biogeochemical model projections at locations of the training set (*Tara* stations). Specificity, *i.e.* the capacity of the model to correctly project absences is represented in function of sensitivity, *i.e.* the capacity of the model to correctly project presences for each MAG for which a valid environmental niche was found. Two thresholds for presence detection are used (in green $p>0.5$, in red $p>0.3$).

Globally, models perform well, especially for $p>0.3$ as a presence threshold, with a vast majority of models with sensitivity >0.6 and specificity >0.6 (61% for $p>0.3$, 39% for $p>0.5$). Lowering the presence threshold allows a global increase in sensitivity with a relatively low decrease in specificity (red points versus green points). Some models perform relatively poorly and have low sensitivity. This might be explained by the asymmetry in number of presences compared to absences in the training set (relatively many more absences). In addition, the spatial structure and

resolution as well as the hidden seasonality (10 years climatologies are used) of the biogeochemical models might explain these discrepancies.

#5: Categorizing the 939 TARA Oceans metagenomes.

Our study surveyed a total of 939 TARA Oceans metagenomes (Table S1) that we organized into four cellular size categories (**size 1**: 0.2-5 μ m, **size 2**: 3-20 μ m, **size 3**: 20-200 μ m, **size 4**: 180-2000 μ m) as well as a wider cellular size fraction encompassing all categories considered in our study (**wider size**: 0.8-2000 μ m). The four cellular size categories were well represented across the five oceans and two seas. Overall, 119 stations contained at least 3 out of the 4 cellular size categories, which we defined as **Station subset 1** (757 metagenomes). Using this first subset, SMAGs were assigned a “**cosmopolitan score**” corresponding to the percentage of stations in which they were detected. SMAGs were also assigned a “**cellular size range**” and “**oceanic signal**” using average coverage in each size categories (n=4) for the former and in each ocean and sea (n=7) for the later. Those results are summarized in the tables S3 and S4. Unfortunately, the wider cellular size fraction was missing in the Mediterranean Sea, Red Sea and Indian Ocean, limiting its use to 91 stations from the four remaining oceans, which we defined as **Station subset 2** (130 metagenomes). Critically, this second subset offers a glimpse into the relative proportion of planktonic lineages of different cellular sizes. While more limited in its geographic scope, the **Station subset 2** could provide important insights into the “**relative proportion**” of SMAGs in stations from the Atlantic, Pacific, Arctic and Southern Ocean.

#6: Manual curation of the DNA-dependent RNA polymerase genes for SMAGs and METdb.

An eukaryotic dataset (Da Cunha)¹⁴ was used to build HMM profiles for the two largest subunits of the DNA-dependent RNA polymerase (RNAP-a and RNAP-b). These two HMM profiles were incorporated within the anvi'o framework to identify RNAP-a and RNAP-b genes (Prodigal⁴ annotation) in the SMAGs and METdb transcriptomes.

We independently performed the following workflow for RNAP-a sequences identified in the SMAGs (round A, n= 1,626) and METdb (round B, n= 2,823) as well as for RNAP-b sequences identified in the SMAGs (round C, n= 1,373) and METdb (round D, n= 3,941):

- (1) **Stetting the stage with references:** Reference sequences for the relevant largest subunits of the DNA-dependent RNA polymerase (e.g., RNAP-a for round A) corresponding to eukaryotic (types I, II and III), bacterial and archaeal lineages from the Da Cunha dataset were added to the sequences identified by the HMM.

- (2) **Phylogenetic tree Phase 1:** Sequences were aligned using the iterative FFT-NS-i refinement method of MAFFT¹⁵ v7.464 with default parameters, and the sites with more than 50% of gaps were trimmed using Galign v0.3.0-alpha5. Phylogenetic trees were reconstructed with IQ-TREE¹⁶ v1.6.12. The model of evolution was estimated with the ModelFinder Plus option¹⁷, and supports were computed from 1,000 replicates for the Shimodaira-Hasegawa (SH)-like approximation likelihood ratio (aLRT)¹⁸ and ultrafast bootstrap approximation (UFBoot)¹⁹. Anvi'o v6.1 was used to visualize and root the phylogenetic trees.
- (3) **Identifying sequences of type I, II and III:** We used the anvi'o interactive interface to root the tree between Bacteria and the rest, and identify sequences corresponding to eukaryotic DNA-dependent RNA polymerase of type I, II and III. Sequences not clearly belonging to one of these three clusters were discarded. Note that during this process other types of eukaryotic RNA polymerase (e.g., nucleomorphs) were identified and put aside for investigations beyond the scope of this study.
- (4) **Fusing fragmented sequences when needed:** For each SMAG or METdb transcriptome, sequences corresponding to the same RNA polymerase type (e.g., RNAP-a_type_I for round A) were aligned against each other and against a relevant eukaryotic reference sequence using blastp²⁰. Non-overlapping sequences corresponding to the same subunit (based on **Phylogenetic tree Phase 1**) were considered fragments of the same gene and fused manually, overcoming fragmentation issues during gene calling and/or transcription. In addition, only the longest sequence was kept for overlapping isoforms and closely related duplicates (>95% identity and >30% coverage).
- (5) **Phylogenetic tree Phase 2:** A phylogenetic tree was performed for each subunit (DNA-dependent RNA polymerase of type I, II and III) as done for the **Phylogenetic tree Phase 1** (for improved resolution, archaeal references were used as outgroup and bacterial sequences removed in this analysis). Distantly related duplicates (those occurred in <5% of SMAGs and <10% of METdb transcriptomes, possibly due to contamination) were carefully considered in the context of the three phylogenetic trees as well as taxonomy to identify and remove sequences with incoherent phylogenetic and/or taxonomic signal.
- (6) **Final collection:** We removed sequences shorter than 200 amino-acids, providing a final collection of DNA-dependent RNA polymerase genes for the SMAGs (n=2,150) and METdb (n=2,032) with no duplicates.

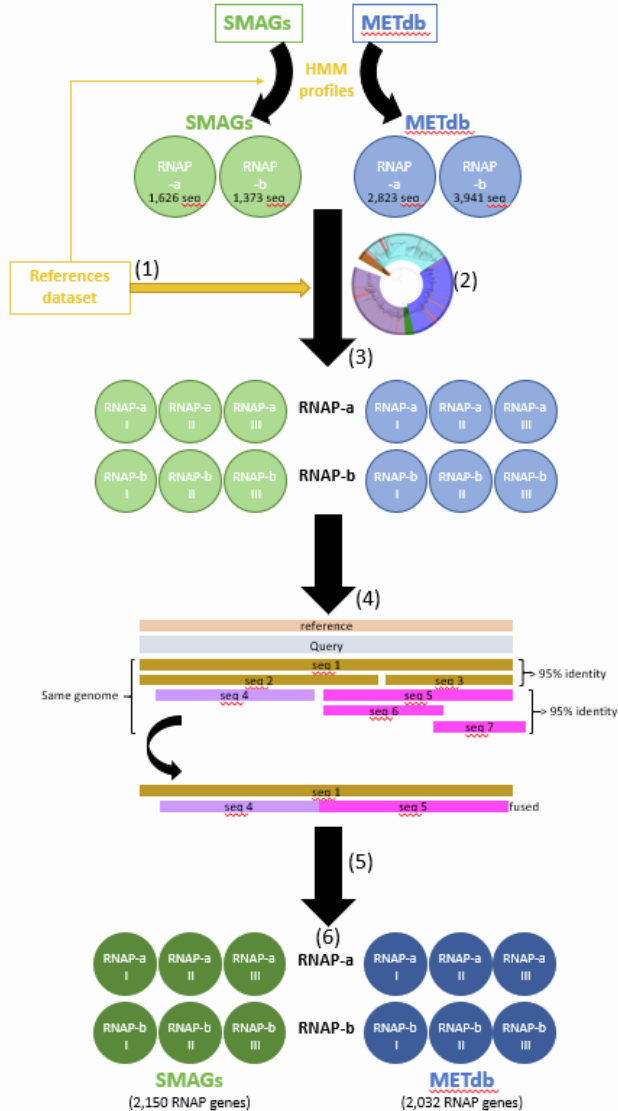


Figure S21: Workflow for the manual curation of RNA polymerase genes identified in the MAGs, SAGs and METdb culture transcriptomes.

References

1. Delmont, T.O. (2018). Assessing the completion of eukaryotic bins with anvi'o. Blog post. <http://merenlab.org/2018/05/05/eukaryotic-single-copy-core-genes/>.
2. Simão, F.A., Waterhouse, R.M., Ioannidis, P., Kriventseva, E. V., and Zdobnov, E.M. (2015). BUSCO: assessing genome assembly and annotation completeness with single-copy orthologs. *Bioinformatics* 31, 3210–3212.
3. Eren, A.M., Esen, Ö.C., Quince, C., Vineis, J.H., Morrison, H.G., Sogin, M.L., and Delmont, T.O. (2015). Anvi'o: an advanced analysis and visualization platform for 'omics data. *PeerJ* 3, e1319.
4. Hyatt, D., Chen, G.-L., Locascio, P.F., Land, M.L., Larimer, F.W., and Hauser, L.J.

- (2010). Prodigal: prokaryotic gene recognition and translation initiation site identification. *BMC Bioinformatics* *11*, 119.
5. West, P.T., Probst, A.J., Grigoriev, I. V., Thomas, B.C., and Banfield, J.F. (2018). Genome-reconstruction for eukaryotes from complex natural microbial communities. *Genome Res.* *28*, gr.228429.117.
 6. Delmont, T.O., Quince, C., Shaiber, A., Esen, Ö.C., Lee, S.T., Rappé, M.S., MacLellan, S.L., Lücker, S., and Eren, A.M. (2018). Nitrogen-fixing populations of Planctomycetes and Proteobacteria are abundant in surface ocean metagenomes. *Nat. Microbiol.* *2018* *37* *3*, 804–813.
 7. Alneberg, J., Bjarnason, B.S., de Bruijn, I., Schirmer, M., Quick, J., Ijaz, U.Z., Lahti, L., Loman, N.J., Andersson, A.F., and Quince, C. (2014). Binning metagenomic contigs by coverage and composition. *Nat. Methods* *11*, 1144–1146.
 8. Sieracki, M.E., Poulton, N.J., Jaillon, O., Wincker, P., de Vargas, C., Rubinat-Ripoll, L., Stepanauskas, R., Logares, R., and Massana, R. (2019). Single cell genomics yields a wide diversity of small planktonic protists across major ocean ecosystems. *Sci. Reports* *2019* *91* *9*, 1–11.
 9. Seeleuthner, Y., Mondy, S., Lombard, V., Carradec, Q., Pelletier, E., Wessner, M., Leconte, J., Mangot, J.F., Poulain, J., Labadie, K., et al. (2018). Single-cell genomics of multiple uncultured stramenopiles reveals underestimated functional diversity across oceans. *Nat. Commun.* *2018* *91* *9*, 1–10.
 10. Mangot, J.F., Logares, R., Sánchez, P., Latorre, F., Seeleuthner, Y., Mondy, S., Sieracki, M.E., Jaillon, O., Wincker, P., Vargas, C. De, et al. (2017). Accessing the genomic information of unculturable oceanic picoeukaryotes by combining multiple single cells. *Sci. Reports* *2017* *71* *7*, 1–12.
 11. López-Escardó, D., Grau-Bové, X., Guillaumet-Adkins, A., Gut, M., Sieracki, M.E., and Ruiz-Trillo, I. (2017). Evaluation of single-cell genomics to address evolutionary questions using three SAGs of the choanoflagellate *Monosiga brevicollis*. *Sci. Reports* *2017* *71* *7*, 1–14.
 12. Vannier, T., Leconte, J., Seeleuthner, Y., Mondy, S., Pelletier, E., Aury, J.M., De Vargas, C., Sieracki, M., Iudicone, D., Vaultot, D., et al. (2016). Survey of the green picoalga *Bathycoccus* genomes in the global ocean. *Sci. Reports* *2016* *61* *6*, 1–11.
 13. Keeling, P.J., Burki, F., Wilcox, H.M., Allam, B., Allen, E.E., Amaral-Zettler, L.A., Armbrust, E.V., Archibald, J.M., Bharti, A.K., Bell, C.J., et al. (2014). The Marine Microbial Eukaryote Transcriptome Sequencing Project (MMETSP): Illuminating the Functional Diversity of Eukaryotic Life in the Oceans through Transcriptome Sequencing. *PLOS Biol.* *12*, e1001889.
 14. Da Cunha, V., Gaia, M., Nasir, A., and Forterre, P. (2018). Asgard archaea do not close the debate about the universal tree of life topology. *PLOS Genet.* *14*, e1007215.
 15. Katoh, K., and Standley, D.M. (2013). MAFFT Multiple Sequence Alignment Software Version 7: Improvements in Performance and Usability. *Mol. Biol. Evol.* *30*, 772–780.
 16. Nguyen, L.T., Schmidt, H.A., Von Haeseler, A., and Minh, B.Q. (2015). IQ-TREE: A Fast and Effective Stochastic Algorithm for Estimating Maximum-Likelihood Phylogenies. *Mol. Biol. Evol.* *32*, 268–274.

17. Kalyaanamoorthy, S., Minh, B.Q., Wong, T.K.F., Von Haeseler, A., and Jermini, L.S. (2017). ModelFinder: fast model selection for accurate phylogenetic estimates. *Nat. Methods* 2017 146 14, 587–589.
18. Guindon, S., Dufayard, J.F., Lefort, V., Anisimova, M., Hordijk, W., and Gascuel, O. (2010). New algorithms and methods to estimate maximum-likelihood phylogenies: Assessing the performance of PhyML 3.0. *Syst. Biol.* 59, 307–321.
19. Hoang, D.T., Chernomor, O., Von Haeseler, A., Minh, B.Q., and Vinh, L.S. (2018). UFBoot2: Improving the Ultrafast Bootstrap Approximation. *Mol. Biol. Evol.* 35, 518–522.
20. Altschul, S.F., Gish, W., Miller, W., Myers, E.W., and Lipman, D.J. (1990). Basic local alignment search tool. *J. Mol. Biol.* 215, 403–410.
21. Boyer, T.P., Antonov, J.I., Baranova, O.K., Coleman, C., Garcia, H.E., Grodsky, A., Johnson, D.R., Locarnini, R. a, Mishonov, A. V, O’Brien, T.D., et al. (2013). WORLD OCEAN DATABASE 2013, NOAA Atlas NESDIS 72. Sydney Levitus, Ed.; Alexey Mishonoc, Tech. Ed.
22. Aumont, O., Ethé, C., Tagliabue, A., Bopp, L., and Gehlen, M. (2015). PISCES-v2: An ocean biogeochemical model for carbon and ecosystem studies. *Geosci. Model Dev.* 8, 2465–2513.
23. Moore, C.M., Mills, M.M., Arrigo, K.R., Berman-Frank, I., Bopp, L., Boyd, P.W., Galbraith, E.D., Geider, R.J., Guieu, C., Jaccard, S.L., et al. (2013). Processes and patterns of oceanic nutrient limitation. *Nat. Geosci* 6, 701–710.
24. Dormann, C.F., Elith, J., Bacher, S., Buchmann, C., Carl, G., Carré, G., Marquéz, J.R.G., Gruber, B., Lafourcade, B., Leitão, P.J., et al. (2013). Collinearity: a review of methods to deal with it and a simulation study evaluating their performance. *Ecography (Cop.)*. 36, 27–46.
25. Brun, P., Kiørboe, T., Licandro, P., and Payne, M.R. (2016). The predictive skill of species distribution models for plankton in a changing climate. *Glob. Chang. Biol.* 22, 3170–3181.
26. Redfield, A. (1934). On the Proportions of Organic Derivatives in Sea Water and Their Relation to the Composition of Plankton. James Johnstone Meml. Vol. Univ. Press Liverpool, 176–192.
[https://www.scirp.org/\(S\(351jmbntvnsjt1aadkposzje\)\)/reference/ReferenceSPapers.aspx?ReferenceID=1883475](https://www.scirp.org/(S(351jmbntvnsjt1aadkposzje))/reference/ReferenceSPapers.aspx?ReferenceID=1883475).
27. van Vuuren, D.P., Edmonds, J., Kainuma, M., Riahi, K., Thomson, A., Hibbard, K., Hurtt, G.C., Kram, T., Krey, V., Lamarque, J.F., et al. (2011). The representative concentration pathways: An overview. *Clim. Change* 109, 5–31.
28. Michelangeli, P.A., Vrac, M., and Loukos, H. (2009). Probabilistic downscaling approaches: Application to wind cumulative distribution functions. *Geophys. Res. Lett.* 36.
29. Ridgeway, G. (2006). Generalized boosted regression models. *Doc. R Packag. “gbm”*, version.
30. Breiman, L., and Cutler, A. (2012). Breiman and Cutler’s random forests for classification and regression. *Packag. “randomForest.”*
31. Venables, W.N., and Ripley, B.D. (2002). *Modern Applied Statistics with S* Fourth edition by.
32. Wood, S.N. (2004). Stable and efficient multiple smoothing parameter

- estimation for generalized additive models. *J. Am. Stat. Assoc.*
33. Biecek, P. (2018). Dalex: Explainers for complex predictive models in R. *J. Mach. Learn. Res.*, 1–5.
 34. Jones, M.C., and Cheung, W.W.L. (2015). Multi-model ensemble projections of climate change effects on global marine biodiversity. *ICES J. Mar. Sci.* 72, 741–752.